AD NUMBER

AD857775

LIMITATION CHANGES

TO:

Approved for public release; distribution is unlimited.

FROM:

Distribution: Further dissemination only as directed by Wright Air Development Center, Wright-Patterson AFB, OF 45433, JUN 1952, or higher DoD authority.

AUTHORITY

AFSC ltr 2 Mar 1972

WADC TECHNICAL REPORT 52-140
pt. 1

A CRITICAL EVALUATION OF THE BORON HARDENABILITY EFFECT IN STEEL

JOSEPH W. SPRETNAK
RUDOLPH SPEISER

THE OHIO STATE UNIVERSITY

JUNE 1952

WRIGHT AIR DEVELOPMENT CENTER

NOTICES

When Government drawings, specifications, or other data are used for any purpose other than in connection with a definitely related Government procurement operation, the United States Government thereby incurs no responsibility nor any obligation whatsoever; and the fact that the Government may have formulated, furnished, or in any way supplied the said drawings, specifications, or other data, is not to be regarded by implication or otherwise as in any manner licensing the holder or any other person or corporation, or conveying any rights or permission to manufacture, use, or sell any patented invention that may in any way be related thereto.

The information furnished herewith is made available for study upon the understanding that the Government's proprietary interests in and relating thereto shall not be impaired. It is desired that the Judge Advocate (WCJ), Wright Air Development Center, Wright-Patterson Air Force Base, Ohio, be promptly notified of any apparent conflict between the Government's proprietary interests and those of others.

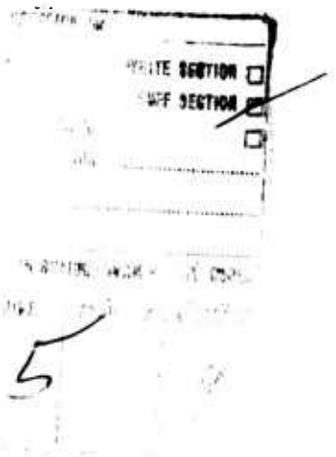

D-1800.

DEPARTMENT OF THE AIR FORCE
HEADQUARTERS AERONAUTICAL SYSTEMS DIVISION (AFSC)
WRIGHT-PATTERSON AIR FORCE BASE, OHIO 45433

REPLY TO ATTN OF: ASNPD

20 J une 1969

SUBJECT: WADC TR 52-140 (TI-2019) Pt 1

TO: AFML (MAAM)

In accordance with instructions from Hq AFSC (SCG), the holdings of the former ASNPD Library are being offered to the Defense Documentation Center (DDC). DDC has indicated an interest in subject document. Request return of report with information as indicated below by.....7 July 1969....

FLOYD H. MASON, Lt Colonel, USAF
Director of Engineering Standards

1 Atch
Subject Report

26 JUN 1969

1st Ind (AFML (MAAM)

TO: ASNPD

1. ASNPD is (is not) authorized to release subject report to DDC. Please underline one.

2. Number of applicable AFR 310-2 distribution statement ..5..... (If none, please check - ☐. If addition or change of statement occurs, please mark it on the report.)

EDWARD DUGGER
Materials Information Branch
Materials Support Division
Air Force Materials Laboratory

1 Atch
Subject Report

AFML/MAAM
W-8 AFB Ohio 45433

(18) WADC (19) TR-52-140-Pt-1

(9)

WADC TECHNICAL REPORT 52-140 pt. 1.

WADC-52-140 AD 10613

(6)

A CRITICAL EVALUATION OF THE BORON HARDENABILITY EFFECT IN STEEL.

(10) Joseph W. Spretnak
Rudolph Speiser

The Ohio State University

(11) June 1952 (12) 86 p.

(15) *Flight Research Laboratory*
Contract No. AF 18(600)-94
RDO No. 463-8-4

Wright Air Development Center
Air Research and Development Command
United States Air Force
Wright-Patterson Air Force Base, Ohio

FOREWORD

This report was prepared by the Metallurgy Department of The Ohio State University as an activity of The Ohio State University Research Foundation. The cooperator is the Air Research and Development Command under Contract No. AF 18 (600) - 94, Research Development Order No. 463 - 8-4, Metallurgy of Boron in Iron and Steel. The research was initiated by and is under the direction of the Flight Research Laboratory, Wright-Patterson Air Force Base, Major A. A. Marston acting as project engineer.

The report was prepared by Professors J. W. Spretnak and Rudolph Speiser, and Mr. C. C. McBride of the Department of Metallurgy, The Ohio State University.

ABSTRACT

The chemistry of boron and the metallurgy of boron in iron and steel are thoroughly reviewed. On the basis of critical evaluation of the existing information, a working hypothesis for the mechanism of the boron hardenability effect is presented. The principal effect of boron is to retard the formation of pro-eutectoid ferrite which forms from austenite by a shear mechanism. This retardation occurs because of the excessively high strain energy peaks associated with boron atoms dissolved in austenite. Nucleation and growth processes are expected only when the system passes from a disordered state to a more highly ordered state.

PUBLICATION REVIEW

The publication of this report does not constitute approval by the Air Force of the findings or the conclusions contained therein. It is published only for the exchange and stimulation of ideas.

FOR THE COMMANDING GENERAL:

LESLIE B. WILLIAMS
Colonel, USAF
Chief, Flight Research Laboratory
Directorate of Research

TABLE OF CONTENTS

TABLE OF CONTENTS (cont'd.)

LIST OF ILLUSTRATIONS

LIST OF ILLUSTRATIONS (cont'd.)

I. REVIEW OF THE METALLURGY AND CHEMISTRY OF BORON

A. INTRODUCTION

1. The Role of Boron in Heat Treatable Steels. A critical shortage of alloying elements such as nickel, chromium, molybdenum, and manganese has resulted from the increased production of high-temperature alloys and alloy steels. Boron as an alloying element in heat treatable steels can substitute for the hardenability effects of the above named alloys. It has been established that as little as 0.0005% boron significantly enhances the hardenability.

Numerous investigations have contributed to the knowledge and "art" of producing and treating boron steels. However, there are many problems to be solved such as effect of steel composition, heat treating variables, mechanism of boron effect, and meaning of effective and ineffective boron. Solution of these problems will lead to a more intelligent use and better control of boron as an alloying element.

2. Brief Historical Review. The first systematic study of boron additions to steel was conducted by Guillet[1] in 1907. Boron additions of 0.1% to approximately 1.5% were added to steels containing from 0.2% to 0.5% carbon. Guillet concluded that boron steels might prove commercially feasible if used in the quenched state.

Some further investigations were conducted using boron in amounts greater than 0.1% but the resulting product was usually brittle and could not be worked[2]. Walters was evidently the first person to recognize the effects of small additions of boron. He obtained German patent rights in 1921 and United States patents[3] in 1924 to cover the addition of boron ranging from 0.001% to about 0.1%.

The first use of boron steels in the United States is rather vague. It appears that International Harvester found a remarkable increase in hardenability which could not be attributed to the components reported[4]. This effect was traced to the presence of boron in the Grainal addition which renewed the interest in boron steels.

During the Second World War and the accompanying shortage of alloying elements, the interest in boron steels was stimulated. By the end of the war some standard boron steels were developed which a few companies continued to produce although the majority of the industry reverted to standard alloying elements. The present emergency has again intensified the interest in boron steels. Furthermore, it has resulted in a trend to produce a material for a certain specification rather than using a material which is over alloyed.

B. FUNDAMENTAL ASPECTS OF BORON AND BORON STEELS

1. Structure and Properties of Boron. In order to evaluate the effect of boron as an alloying element, some fundamental information in regards to its structure and properties should be considered. Unfortunately, although boron is relatively abundant, very little is known about this element. However, some studies are being conducted in regards to the crystal structure and these results will be considered first.

The main problem encountered in the study of the properties and crystal structure of boron was the preparation of the pure material. Laubengayer, et al[7], review the methods used in preparing pure boron and state that the thermal decomposition of boron tribromide was the most satisfactory process. Laubengayer, et al[8], discussed the investigation of pure boron produced in this manner.

Boron resulting from hydrogen reduction of boron tribromide (BBr_3) was condensed on a hot filament of tungsten or tantalum. The crystalline nature of the condensed boron was dependent on the concentration of BBr_3 and particularly on the filament temperature. Deposits ranged from amorphous, to vitreous, to crystalline with increasing filament temperature and decreasing BBr_3 concentration. Two types of crystals are observed, (1) "needle-like" and (2) "plate-like" crystals. The x-ray patterns of these two crystals are different. Preliminary work indicated the latter to be orthogonal and the needle-like crystals as tetragonal. The smallest cell based on orthogonal axes for the plate crystals has a = 17.86Å; b = 8.93Å; c = 10.13Å. Determination of the density of the needle crystals yielded 2.310 gm/cc which agrees closely with previous determinations.

Complete (CuK_α) Weissenberg photographic x-ray data of the needle crystals has been recently reported[9]. These data establish a tetragonal unit cell with a = 8.73 ± 0.02Å, and c = 5.03 ± 0.02Å containing 50 atoms. These authors state that further study is being conducted to determine the space group and that investigation of the plate crystals is being continued.

Johnston, Hersh, and Kerr[10] prepared amorphous boron by the thermal decomposition of diborane (B_2H_6). This high purity amorphous boron was compacted and recrystallized. The "d" values obtained from x-ray data agreed well with those reported above.

A few of the physical properties of boron reported by Laubengayer[7] are given below:

Chemical - Boron is extremely inert, it was unaffected by boiling hydrochloric acid or by hydrofluoric acid. It is not easily oxidized in the crystalline state. The hardness of boron approaches that of boron carbide which is the second hardest material in the crystalline state.

Electrical - Boron exhibits a microphonic effect similar to carbon. Experiments indicate that it is a poor electrical conductor.

Optical - Boron is opaque with a black, metallic sheen. It is slightly transparent to a strong arc with a condensing lens.

Godfrey and Warren[11] determined the coordination scheme of boron by a Fourier integral analysis of the powder pattern and estimated six nearest neighbors at an average distance of 1.89Å.

Wells[12] states that boron has little in common with the other elements in Group III (B, Al, Sc, Y, La, Tl, Ac). It is the most electronegative element of the group and in general resembles the non-metals, particularly silicon. Boron forms either three coplanar bonds with interbond angles of 120° or four tetrahedral bonds. The three bonds utilize one 2s and two 2p orbitals which presumably is some kind of hybrid sp^2 orbital.

Seitz[13] lists boron as the second highest electropositive element of the non-metallic elements with hydrogen being first.

2. Structure and Properties of Borides. In order to better understand the behavior of boron it is of interest to consider the various borides.

Kiessling[14] summarizes the crystal structure of the borides of the transition elements. It is shown that the borides may be classified according to the arrangement of boron atoms. The phases are regarded as metal lattices with boron in the interstices. As the boron content increases, the number of boron-boron bonds increase, ranging from isolated atoms to three dimensional boron networks. The compounds (1) γ (Me_2B) are typical of isolated boron atoms; (2) δ (MeB) are typical of zig-zag chain networks, and (3) (Me_2B_5) or (MeB_2) are typical of hexagonal network and sheets.

Hagg[15] discusses the regularity of crystal structures in hydrides, borides and carbides of transition elements. He states that if the ratio of r_x/r_m is equal to or less than 0.59, the structure is simple. This rule is apparently valid for the borides of the MB type (isolated boron atoms) but is of less importance for the borides which have boron-boron bonds[14,16]. Norton, et al[16] state that the borides have well developed metallic properties. Hannesen[17] reports that iron-boron alloys ranging from 0 - 8.5% boron behaved ferromagnetically. He concludes that the boride Fe_2B is magnetic.

3. Iron-Boron Equilibrium Diagram. In order to gain an understanding of the behavior of boron in steels, it is obvious that the study of the iron-boron system is indispensable. In addition to yielding information in regards to degree of solid solubility, type of solutions (substitutional or interstitial) effect of boron on the transformation points and etc., this binary diagram is a prerequisite for a Fe-B-C ternary study.

Unfortunately, as will be seen below, only the region above 1% boron appears to be in common agreement. Thus, that part of the diagram which is of the most interest in boron steels (less than 0.007% by weight) has not been accurately determined. However, existing data are of interest and do yield some valuable information.

Hannesen[17] determined the Fe-B diagram up to approximately 8.5% boron while Tschischewski and Herdt[18] developed it up to 11.5% boron. These investigations were conducted by thermal analysis and microscopic investigations and the systems are reviewed by Hansen[19].

The results of these studies agree in essentials but differ appreciably in degree of solid solubility. (See Figures 1 and 2). In addition, Hannesen found a stable boride melting at 1350°C which he designated as Fe_5B_2 (7.19% B) whereas Tscheschewski-Herdt found this boride to correspond to the formula Fe_2B (8.83% B) with a melting point of 1325°C.

In regards to equilibrium in the solid state both works agree in the following points: (1) the solubility of boron in gamma iron increases with decreasing temperature; (2) the temperature of the gamma to alpha transformation is lowered by boron; (3) the eutectoid with respect to boron saturated gamma phase decomposes into boride and alpha iron. The solubility of boron in gamma iron is approximately 0.8% boron at 713°C according to Hannesen while Tscheschewski-Herdt found it to be 3.6% boron at 760°C. The latter investigators determined the solubility of boron in alpha iron at the eutectoid temperature as 0.08%.

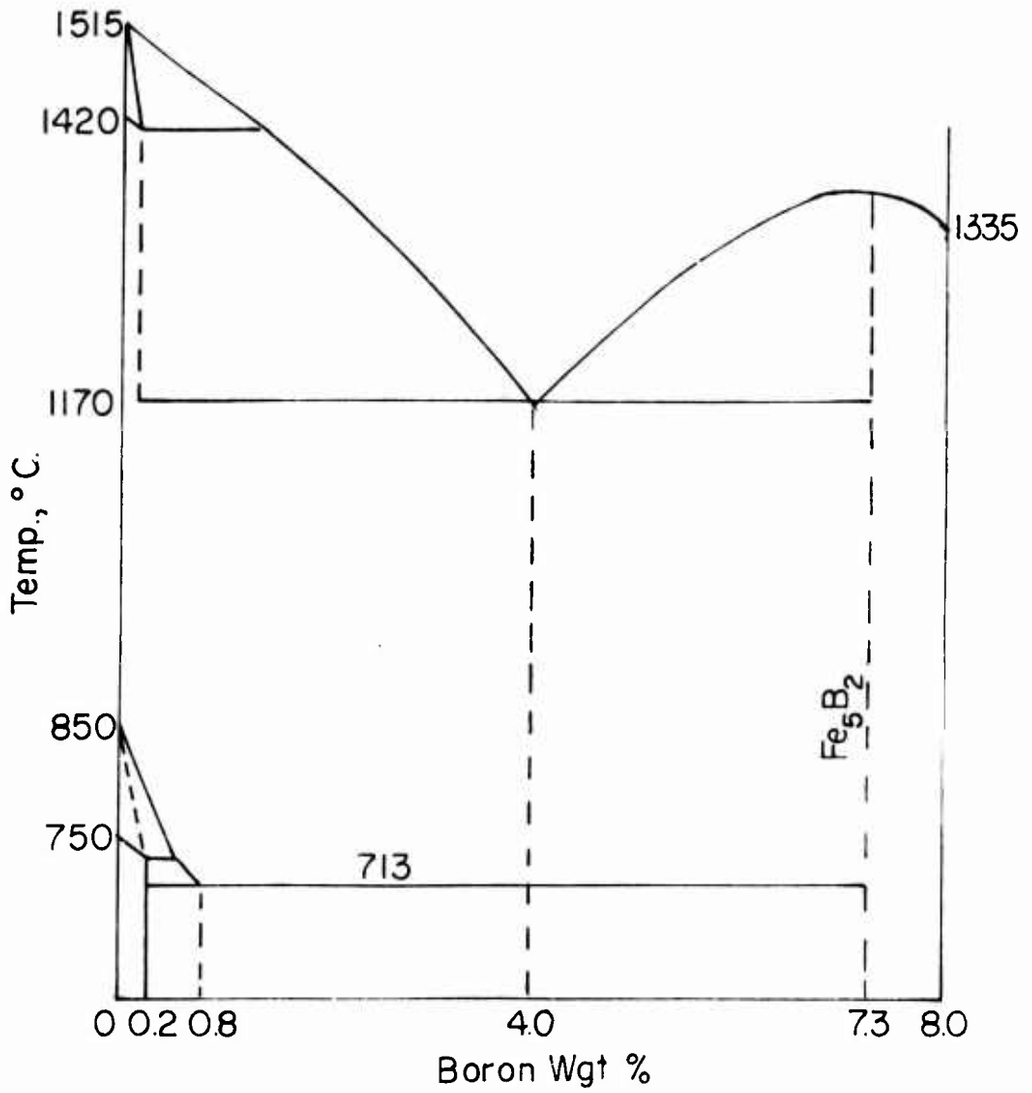

IRON-BORON EQUILIBRIUM DIAGRAM AS DETERMINED BY HANNESEN.

FIGURE 1

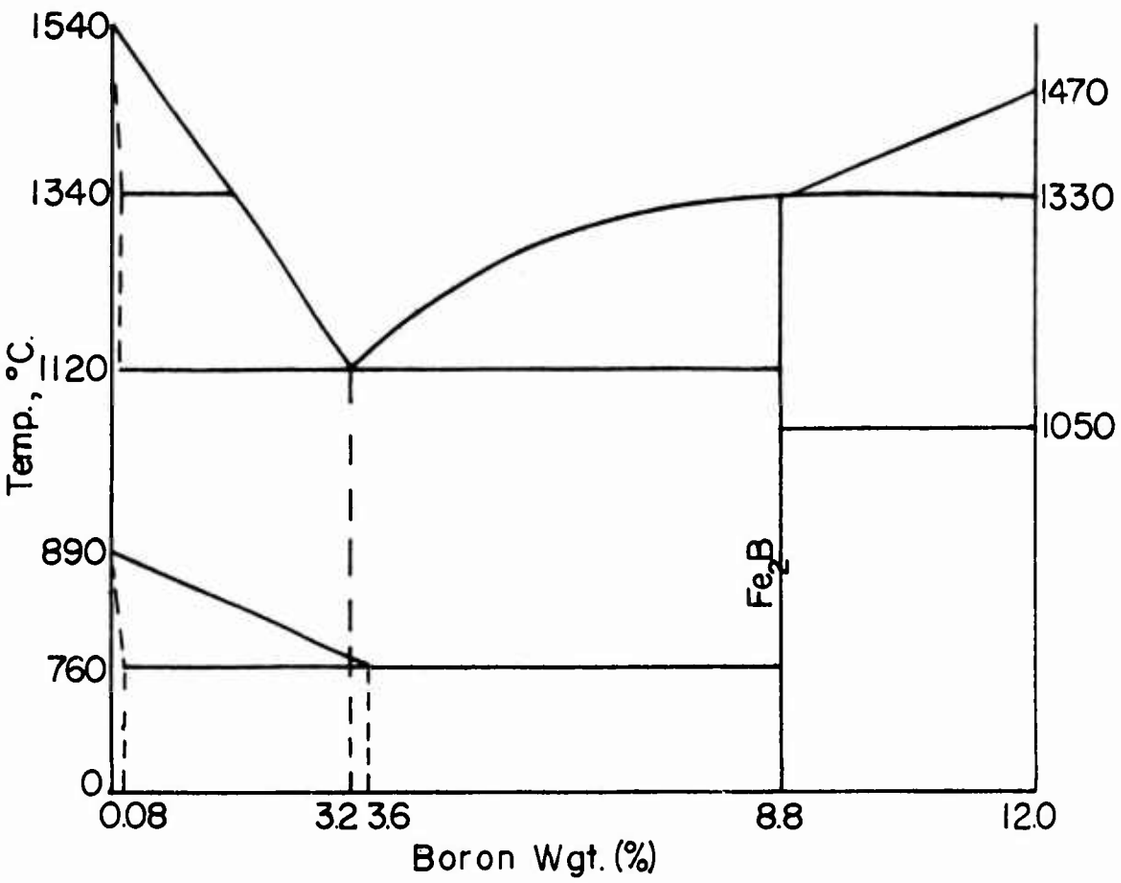

IRON – BORON EQUILIBRIUM DIAGRAM AS DETERMINED BY TSCHISCHEWSKI AND HERDT.

FIGURE 2

The Fe-B equilibrium diagrams determined by the above studies are similar to the Fe-C diagram. Thus, one could conclude that the effect of boron on hardenability is a result of the large difference in solubility between gamma and alpha iron, similar to the effect of carbon.

However, Wever and Mueller[20] pointed out that the results of the two above investigations were in error due to appreciable contamination of carbon, aluminum, and silicon. Carbon was obtained from the carbon-arc furnace and some silicon pick-up resulted from the crucibles used. Furthermore, the ferroboron alloy used contained appreciable aluminum and silicon. These authors state that the effects of boron on the transformations are negligible compared to the effects of these impurities.

Wever and Mueller[20] redetermined the Fe-B diagram with the aid of thermal, microscopic and x-ray studies. These authors prepared their melts in magnesia crucibles using electrolytic iron and the purest ferroboron obtainable at that time. The major impurities in the ferroboron were 0.06% C, 0.89% Si, 0.62% Mn and 4.3% Al. They managed to keep the resultant alloys relatively low in carbon but still obtained some silicon contamination and approximately 1.0% of aluminum. In order to correct for the effects of these impurities, brief studies were made to determine the effects of silicon and aluminum on the transformation points. They concluded that the effects of aluminum and silicon were similar in that these elements restrict the gamma field by lowering A_4 and raising the A_3 transformations. As a result of these studies these authors attempted to correct for the effects of silicon and aluminum and extrapolated to what they term an "idealistic" diagram which is shown in Figure 3.

The solubility of boron, as reported, is very limited and is as follows: (1) at 1381°C in delta iron, 0.15% B; (2) at 1381°C in gamma iron, 0.10% B; (3) at 1174°C in gamma iron, less than 0.15% B; (4) at 915°C in gamma iron, 0.10% B; (5) based on x-ray results the solubility of boron in alpha iron is less than 0.15% at 915°C; (6) at 880°C, 0.10% B. The A_3 temperature is raised by 0.15% boron to 915°C and the peritectic temperature decreases with increasing boron.

Wever and Mueller[20] investigated the x-ray powder patterns of iron-boron alloys containing 0.06% and 0.20% boron. Specimens of these alloys were both slowly cooled and quenched from just below the A_3 transformation (880°C). The slowly cooled specimens produced parameter values which, within the limits of accuracy, could be considered constant. Parameter values derived from the quenched alloys show a contraction of the lattice of alpha iron with increasing boron. Thus, it was concluded that boron forms a substitutional solid solution with alpha iron. To further supplement these findings they studied the patterns of two hypoeutectic alloys with 0.20 and 3.5% boron as well as two hypereutectic alloys with 6.0% and 9.02% boron.

A complete structural analysis of Fe_2B conducted by Wever and Mueller[20] showed that it possesses a body centered tetragonal lattice with four groups of Fe_2B per unit cell. They also determined that FeB exists.

Bjurstrom and Arnfelt[21] confirmed the crystal structure of Fe_2B as well as the composition of FeB (16.23% B). The latter boride has an orthorhombic structure with four groups of FeB in the unit cell. The constancy of the parameters of these borides indicate negligible solubility. The parameters

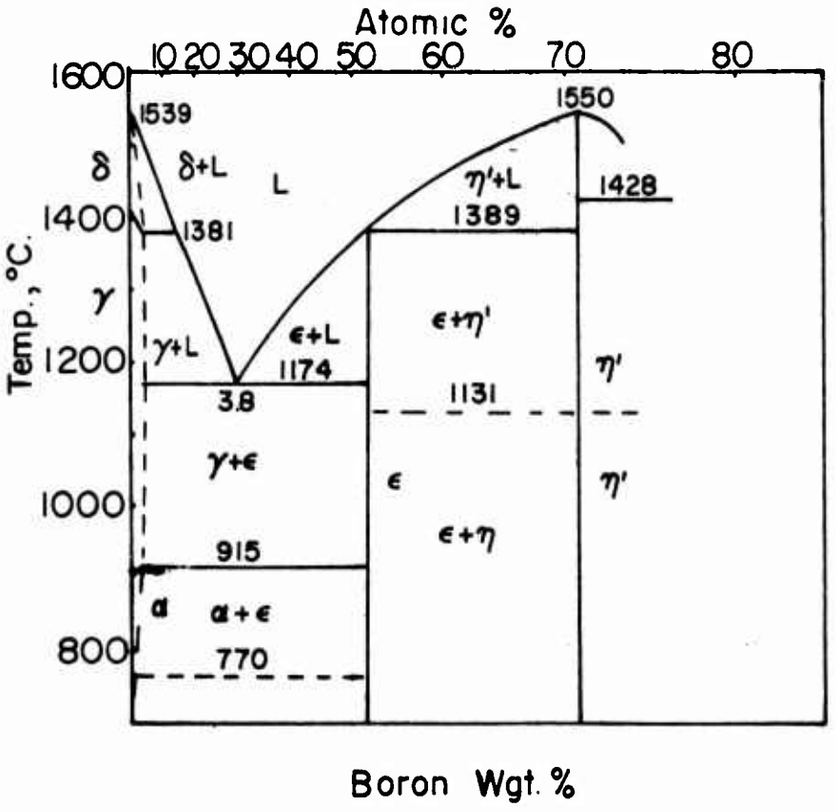

IRON-BORON EQUILIBRIUM DIAGRAM AS DETERMINED BY WEVER AND MÜELLER

FIGURE 3

are as follows:

Fe_2B	Space centered tetragonal	a = 4.240 c = 5.099	Space Group V_{4H}^{18}
FeB	Orthorhombic	a = 2.940 b = 4.05 c = 5.495	

The computed radius of the boron atom ranges from 0.89 to 0.97Å depending upon the crystal structure selected. This yields an average atomic diameter of 1.86Å.

Wasmuht[22] aged five alloys containing from 0.06% to 2.5% boron at several different temperatures after quenching from 750°C. No precipitation was observed which led to the conclusion that the solubility of boron in alpha iron did not decrease below 750°C.

Recent studies on the solid solubility of boron in iron have been conducted by Nicholson[5,6]. Boron was introduced into high purity iron wire by the thermal decomposition of diborane (B_2H_6). This resulted in a layer of Fe_2B and a core of unsaturated iron. These specimens were then annealed for approximately 150 hours and the boron in the core was determined by chemical and spectrographic analyses. These results indicate a peritectoid reaction as shown in Figure 4.

Summarizing the above, the solubility data obtained by Nicholson are without doubt the most valid since the impurities which influenced the results of the previous investigations were minimized.

The data reported by Wever and Mueller in regards to the substitutional solid solution of boron in alpha iron is of doubtful value because of the effects of aluminum and silicon in such a study. Further studies of this type both in alpha and gamma iron are desirable. Particularly, since diffusion data, to be reported below, indicates that boron forms an interstitual solid solution in gamma iron. However, since the data of Nicholson show a greater solubility of boron in alpha iron, one is forced to conclude that boron does in fact form a substitutional solid solution in alpha iron, since the interstitial holes in alpha are much smaller than those in the gamma phase.

4. Iron-Boron-Carbon System. Although the iron apex of the Fe-C-B ternary equilibrium diagram is of extreme interest only two investigations have been reported in literature. In 1922 subsequent to the works of Walters pertaining to the effect of small amounts of boron in steels, Vogel and Tammann[23] studied the Fe-Fe_3C-Fe_2B system.

These authors reviewed the previous Fe-B binarys determined by Hannesen and by Tschischewski and Heßdt and concluded that the latter's work was the best. Thus, with some modifications resulting from theoretical considerations, they assumed the Fe-B system as determined from Tschischewski and Heßdt's data. The pseudo-binary diagram of Fe_2B and Fe_3C resulting from this study is shown in Figure 5.

The development of this ternary was accomplished by thermal analysis and microscopic studies. However, these authors did not record the amounts

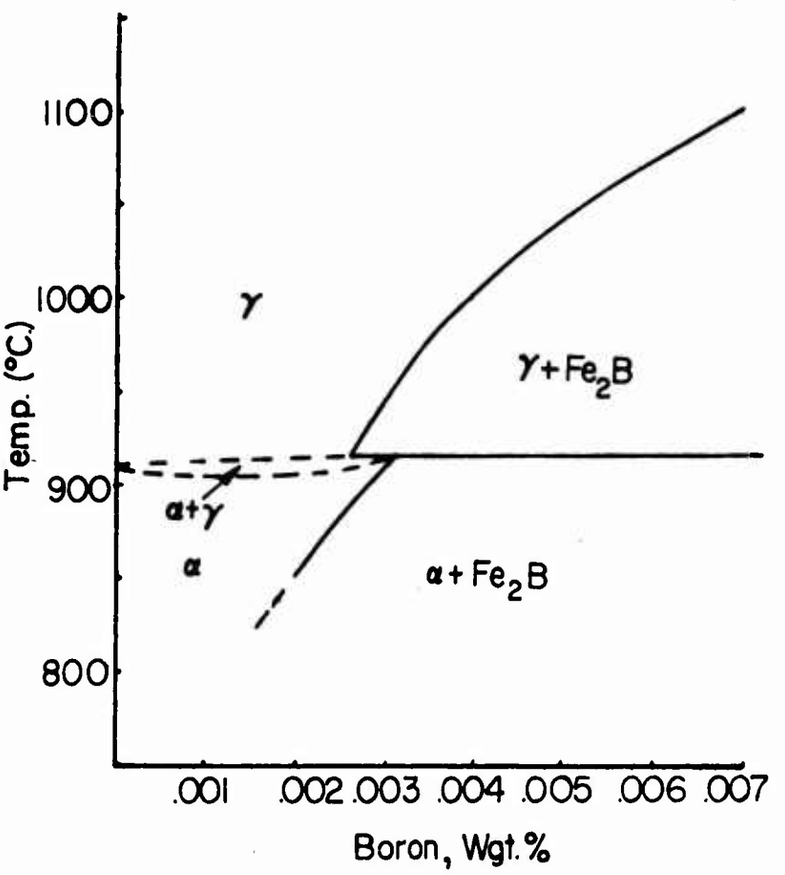

SOLID SOLUBILITY OF BORON IN IRON
AS DETERMINED BY NICHOLSON.

FIGURE 4

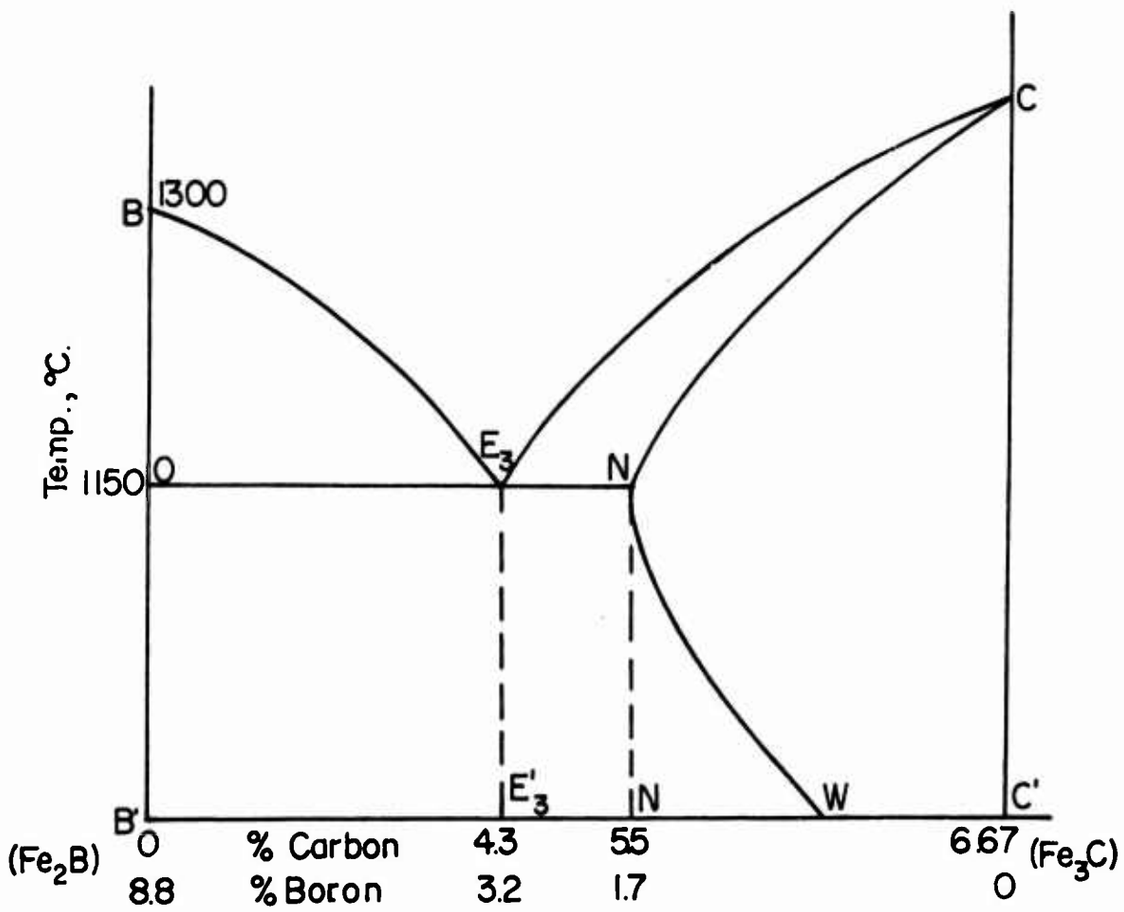

IRON BORIDE - IRON CARBIDE SYSTEM FROM VOGEL AND TAMMANN

FIGURE 5

of impurities such as aluminum and silicon which Wever and Mueller later showed to exert a major influence on the transformations. Vogel and Tammann state that the Fe-B-C alloys were extremely sluggish in approaching equilibrium which casts further doubt as to the validity of their work. However, Figures 6 and 7 show the solid state fields as determined by these authors.

D. S. Clark [24] conducted a metallographic study of the Fe-Fe_3C-Fe_2B system and substantiated the liquid-solid transformations as proposed by Vogel and Tammann. Clark states that the transformations in the solid state were in agreement with Vogel and Tammann's except in the region containing less than one percent boron. The solubility of Fe_2B in alpha iron was less than previously reported unless the alloy contained silicon contents greater than one percent. The ternary diagram showing the ternary eutectic (R') is shown in Figure 8. The melting point of R' is 1100°C. In addition, the boundary of the surfaces of limiting solubility of boron and carbon in gamma iron which terminate in V' along the dotted lines to the level of the ternary eutectic is shown.

The alloys used in this investigation contained boron contents above 0.2% and carbon contents of 0.2 to 3.8%. Thus, the region of the greatest interest in regards to boron steels was not accurately determined and the effect of boron on the accompanying transformations is probably in error.

The above ternary studies are of little value in regards to the study of boron steels. Thus, an investigation of the region at the iron apex is desirable.

5. Diffusion Data. There have been no quantitative data reported in literature on the diffusion of boron in iron although some estimates have been made.

Digges, Irish and Carwile [25] observed a loss of boron in the decarburized zones of commercial steels and state that the rate of diffusion of boron was apparently of the same order of magnitude as that of carbon. In specimens with 0.1% carbon the diffusion of boron was equal to or greater than the diffusion of carbon. These authors calculated the rate of diffusion of boron from the decarburized zone at a temperature of 1038°C as $D = 2.0 \times 10^{-7}$ cm^2/sec. They further state that this indicates that boron is in the interstitual positions of gamma iron. Wells, et al[27], recalculated the diffusion coefficient from the above decarburized specimen as 1.3×10^{-7} cm^2/sec.

Campbell and Fay [26] studied the case hardening effects of boron and nitrogen on a low carbon steel (0.12% C) and concluded that boron penetrates the steel in much the same manner as does carbon under similar conditions. These authors observed that nitrogen is much more readily absorbed by a boron steel than by a carbon steel, which they attribute to the formation of a stable boric nitride. The value for the diffusion coefficient of boron in iron was calculated by Wells, et al [27] from the works of Campbell and Fay and was found to be 3×10^{-7} cm^2/sec. at 900°C.

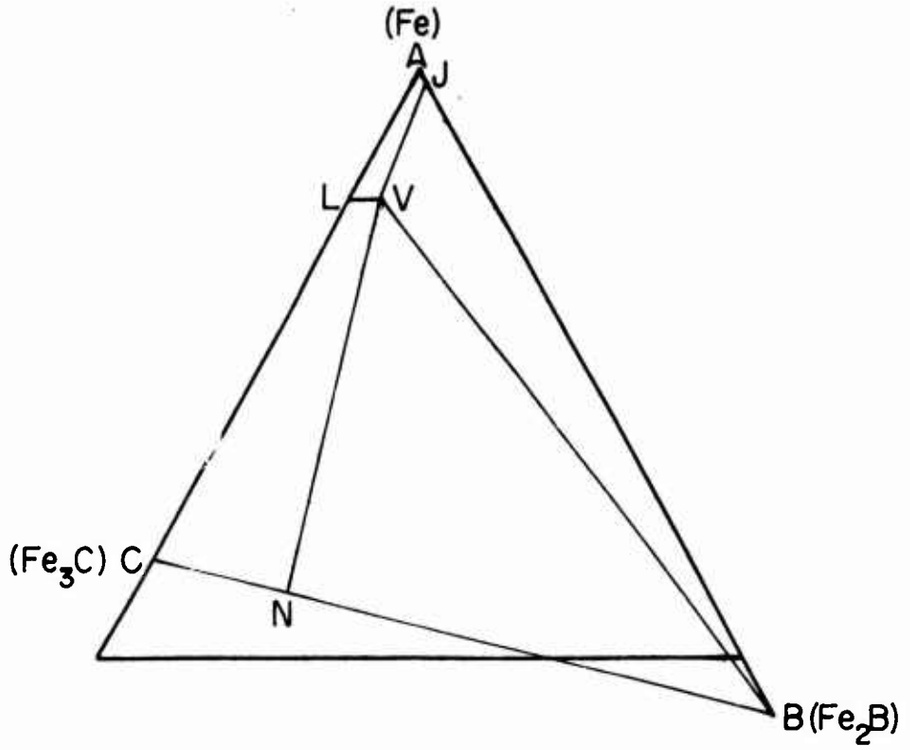

AREA	PHASES
AJVL	1. Unsaturated Ternary Gamma Iron Solid Solution: Maximum Carbon Content 1.9%, Max. Boron 0.3%
LVNC	1. Carbon Saturated Ternary Gamma Iron Solid Solution (LV) 2. Cementite Solid Solution (CN) Carbon 6.6 to 5.3% Boron 0.0 to 1.7%
JVB	1. Boron Saturated Gamma Iron Solid Solution (JV) Carbon 0.0 to 1.6% Boron C.08 to 0.3% 2. Iron Boride - Fe_2B
VNB	1. Carbon and Boron Saturated Ternary Solid Solution (V) 2. Iron Boride - Fe_2B 3. Saturated Cementite Solid Solution (N); Carbon 5.3%; Boron 1.7%

SOLID PHASES - IRON - IRON CARBIDE - IRON BORIDE SYSTEM (GAMMA REGION) [23]

FIGURE 6

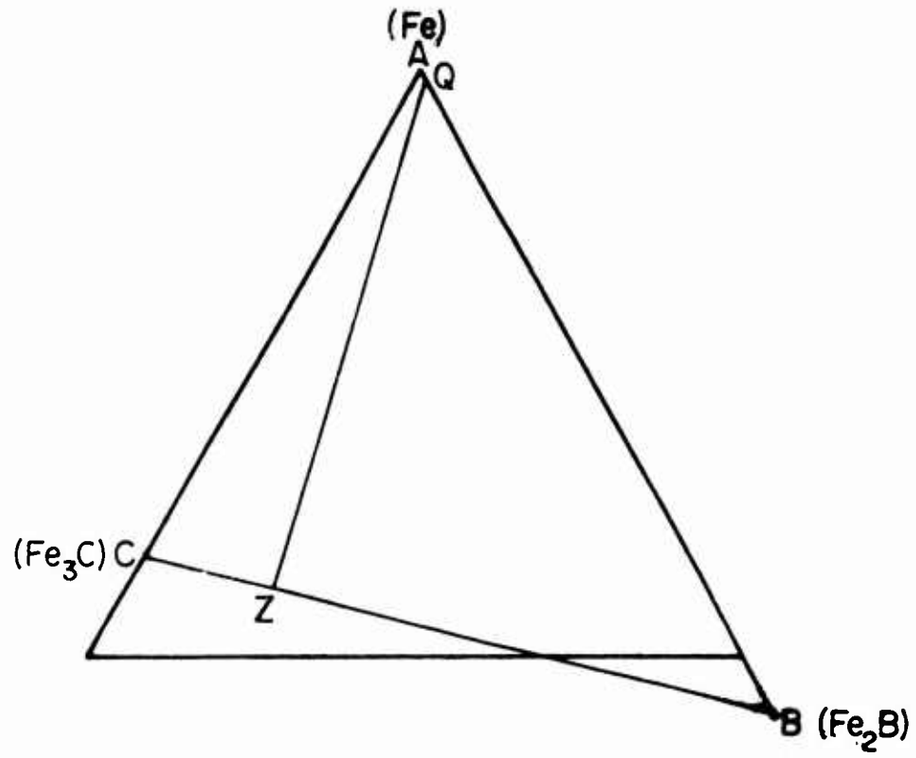

AREA	PHASES
AQZC	1. Binary Alpha Iron Solid Solution (AQ); Boron 0.0 to 0.8% 2. Cementite Solid Solution (CZ)
QZB	1. Saturated Binary Alpha Solid Solution (Q) 2. Iron Boride (Fe_2B) 3. Saturated Cementite Solid Solution (Z); Carbon 5.5%, Boron 1.4%

SOLID PHASES; IRON - IRON CARBIDE - IRON BORIDE SYSTEM (ALPHA REGION)[23]

FIGURE 7

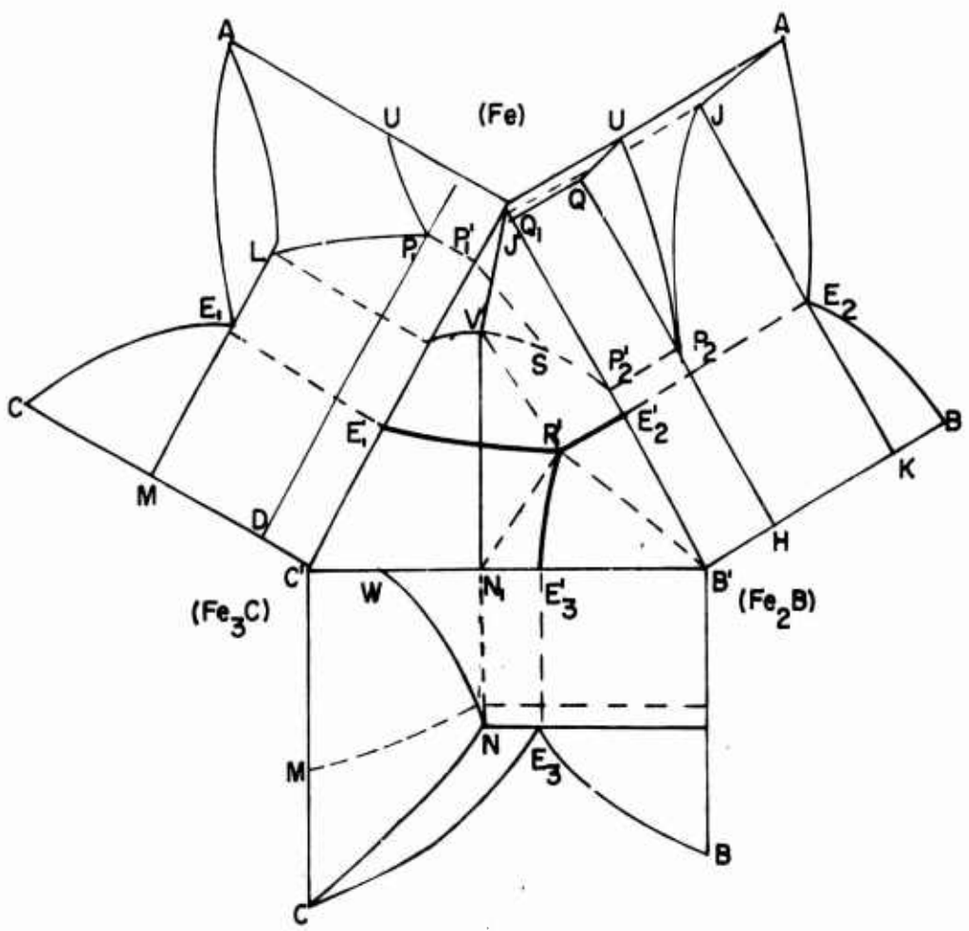

IRON - IRON CARBIDE - IRON BORIDE SYSTEM[23]

FIGURE 8

Kase[29] reports that the diffusion of boron in iron increases abruptly at the A3 point and the rate of diffusion follows the normal effect of increasing with increasing temperature.

Cornelius and Bollenrath[30] studied the migration of boron in steel containing carbon contents from 0.05 to 0.20%. The steel was packed in ferroboron and the diffusion anneal was conducted in a vacuum at 1100°C. The specimens were decarburized and quantitative data could not be obtained. However, these authors state that carbon has a detrimental effect on the diffusion of boron and that boron has a high diffusion rate in iron and in steel.

Wells, Batz and Mehl[31] did not obtain conclusive evidence but state that boron apparently lowers the diffusion coefficient of carbon at 1125°C.

It should be restated that the above values reported for the diffusion coefficients of boron and the effect of boron on the diffusion of carbon are only qualitative data. Interpretation of decarburized specimens is difficult and the interface resulting from packing ferroboron around steel would be very poor. Furthermore, since the studies were conducted on commercial steels, the effects of other elements on the diffusion of carbon and boron cannot be neglected.

Seith and Daur[32] studied the migration of carbon, nitrogen, boron and nickel in iron under the influence of an electrical field. As an introduction to this study these authors state that the conception of conductivity by means of free electrons implies the presence of metal ions in solid metals. Thus, on the passage of a strong current, not only must the electrons migrate to the anode but also the metal ions must migrate in the opposite direction to the cathode. This migration is not detectable in a homogeneous metal since the metal lattice is considered as the system. If, however, the metal phase considered contains two or more components whose mobility and charges are of a particular nature then a state may occur in which the density of the positive charges at the cathode becomes very large. This type of study has been conducted on numerous liquid alloys and some solid alloys and the resultant phenomena must be explained due to the above discussed charge distributions in the crystal.

The principle of this theory is that if equal size atoms are utilized in the erection of the solid solution, then that one with the higher positive charge will strive towards the cathode. In the case of different size atoms with similar charges, the smaller ones migrate to the cathode while the large ones are crowded to the anode. If one subjected a homogeneous solid solution to electrolysis between non-corrodable electrodes, dissolved charged substances such as arise in the electrolysis of aqueous solutions is not expected, but the component under consideration is concentrated with respect to the ends of the system until equilibrium is attained. The forces maintaining the balance are those of the electrolytic transport in the direction of the electrode and the force of diffusion which tries to further equalize the resulting concentration gradients. The theoretical considerations show first the effect of the atomic size which is in agreement with experiments, but it does not predict the possible direction of migration, or the sign of the charge. In many cases, this is just opposite to what one might first expect. In lead, the noble gold

migrates to the anode. Also in copper, the gold goes to the anode. Carbon, which forms a carbide with iron, goes on the other hand, to the cathode.

Results of this study showed that carbon and boron migrated to the cathode whereas nitrogen was transported to the anode. The authors concluded that these results indicate that nitrogen exists in the form of nitride and has taken up electrons. Carbon and boron, on the other hand, are dissolved as ions. This might also be stated as the existence of stronger bonds between nitrogen and iron than between carbon or boron and iron. The diffusion coefficient of boron in iron at approximately 1040°C was estimated from the data to be 1×10^{-5} cm^2/sec. It is of interest that similar studies conducted with nickel or silicon showed no apparent migration.

Dayal and Darken[33] conducted similar tests with some modifications of the technique and observed a migration of carbon to the cathode in agreement with the above authors. However, the difficulty in interpreting the results obtained from migration studies under the influence of an electric field should be considered. Migration of an element to the cathode only implies that the electron configuration of the element, under the influence of an electric field, has become of such a nature as to be positively charged. However, one cannot conclude from these results alone that the electron configuration of the atom in its natural state is similar.

The primary purpose of considering the possible effect of boron on the diffusion of carbon was that it was first thought that such an effect might explain the effect of boron on the hardenability of steel. This thought stemmed from the fundamental fact that the first product of the decomposition of austenite in hypoeutectoid steels is proeutectoid ferrite and in order for ferrite nuclei to exist carbon must diffuse away from this region. If boron in some manner prevented the diffusion of carbon then of course such nuclei could not form and in this manner the decomposition of austenite would be inhibited. As a result of this line of thought, the effects of the common alloying elements such as molybdenum, chromium, nickel, etc. on the diffusion of carbon were briefly reviewed and apparently much confusion exists. Furthermore, very little is apparently known concerning the mechanism of these common alloying elements pertaining to the decomposition of austenite.

However, it is of interest to consider some effects reported in literature. Darken[34] reports on the diffusion studies of carbon in alloy steels containing silicon or manganese. At approximately equal carbon contents carbon diffuses from a high silicon to a low silicon austenite and from a low manganese to a high manganese austenite. Silicon decreases the diffusivity of carbon in austenite whereas equilibrium measurements show that silicon markedly increases the activity coefficient of carbon in austenite.

Wells, Batz and Mehl[31] also found some indication that silicon (2%) lowers the diffusion coefficient of carbon at 1127°C.

Blauter[35] studied the effect of nickel on the diffusion of carbon in austenite at 1000°, 1100°, and 1200°C. He states that the diffusion coefficient of carbon increases continuously with increasing nickel.

Ham, Parke, and Herzig[36] report on the effect of molybdenum on the diffusion rate of carbon. These authors state that at approximately 1093°C, molybdenum has little or no effect on the rate of carbon diffusion. However, at higher temperatures the rate is accelerated while at lower temperatures it is

retarded. They further state that this retardation accounts for only a small part of the effect of molybdenum on hardenability.

Smoluchowski[37] found that at 1000°C both molybdenum and tungsten retard the diffusion of carbon. The effect of tungsten was more than twice that of molybdenum. This author states that there is no connection between the variation in lattice parameter of face-centered-cubic iron and the variation in the diffusion rate of carbon.

6. Effect of Boron on Thermal, Magnetic and Electrical Properties. Early studies of the electrical and magnetic properties of fused boron are summarized by Mellor[76]. It was observed that fused boron at ordinary temperatures is a very poor conductor. Its specific resistivity is 10^{12} times that of copper at ordinary temperatures, a value similar to that of carbon. However, unlike carbon, boron has an abnormally high negative temperature coefficient of resistance as shown in Figure 9. Above 1000°C, the resistance is but a fractional part of an ohm. Studies of fused boron also showed that it behaved somewhat like a spark gap or arc rather than a solid conductor. A breakdown in voltage as in the case of an air gap was observed. (See Figure 10). The fused boron studied was not pure crystalline boron so that the properties reported can only be considered as qualitative data.

Yensen[77] studied the effect of boron upon the magnetic and electrical properties of iron. He found that small additions of boron as boron suboxide (B_7O) had a slightly beneficial effect upon the magnetic properties. This was explained as probably being due to the reduction of iron oxide. This beneficial effect reaches a maximum at small contents and when sufficient amount of boron suboxide was added to leave a measurable quantity of boron combined with the iron a definite detrimental effect of the magnetic properties was observed. Yensen also states the boron increased the specific electrical resistance of iron by 0.62 microhms per 0.1% boron combined with the iron. The purpose of the above study was to find an alloying element which would reduce the last traces of iron oxide and not alloy with the iron. Furthermore the chemical analysis used was not accurate for small amounts of boron so that the data cannot be considered quantitative.

Clark[24] studied the effect of boron on the thermal conductivity of steel and observed a very noticeable decrease as shown in Figure 11. It was observed that the content of graphitic carbon decreased in the same manner.

C. ENGINEERING ASPECTS

1. Deoxidation and Removal of Nitrogen. With the exception of the usual control methods used in processing a good quality steel up to the point where the steel is in the ladle, no other control is indicated for the boron steels. However, the deoxidation practice and the fixation of nitrogen are of extreme importance because of the high affinity of boron for these elements. Ignorance of this fact can probably explain the failure of early investigators to obtain the boron effect at small boron additions and the confusion that existed relative to the required amounts of boron.

Udy and Rosenthal[39] found that full deoxidation of the melt was required to avoid inconsistent hardenability results.

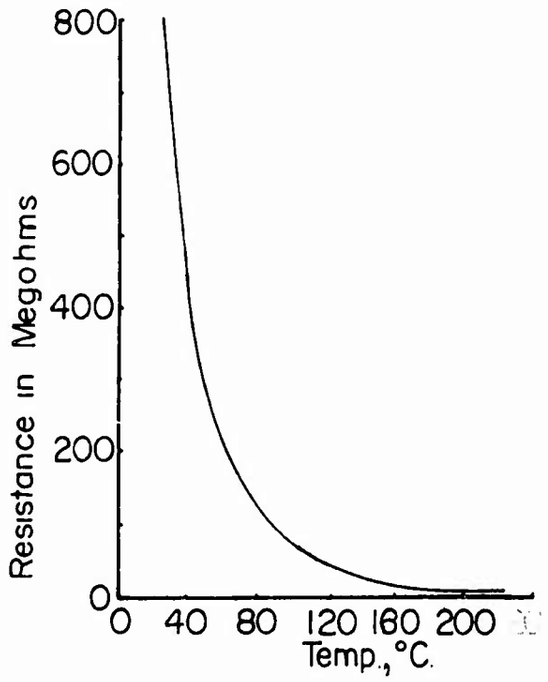

RESISTANCE OF BORON VS. TEMPERATURE [76]

FIGURE 9

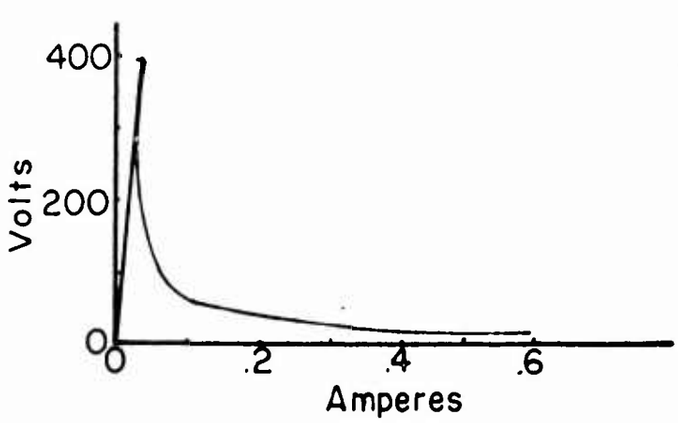

VOLT-AMPERE CURVE OF BORON IN AIR [76]

FIGURE 10

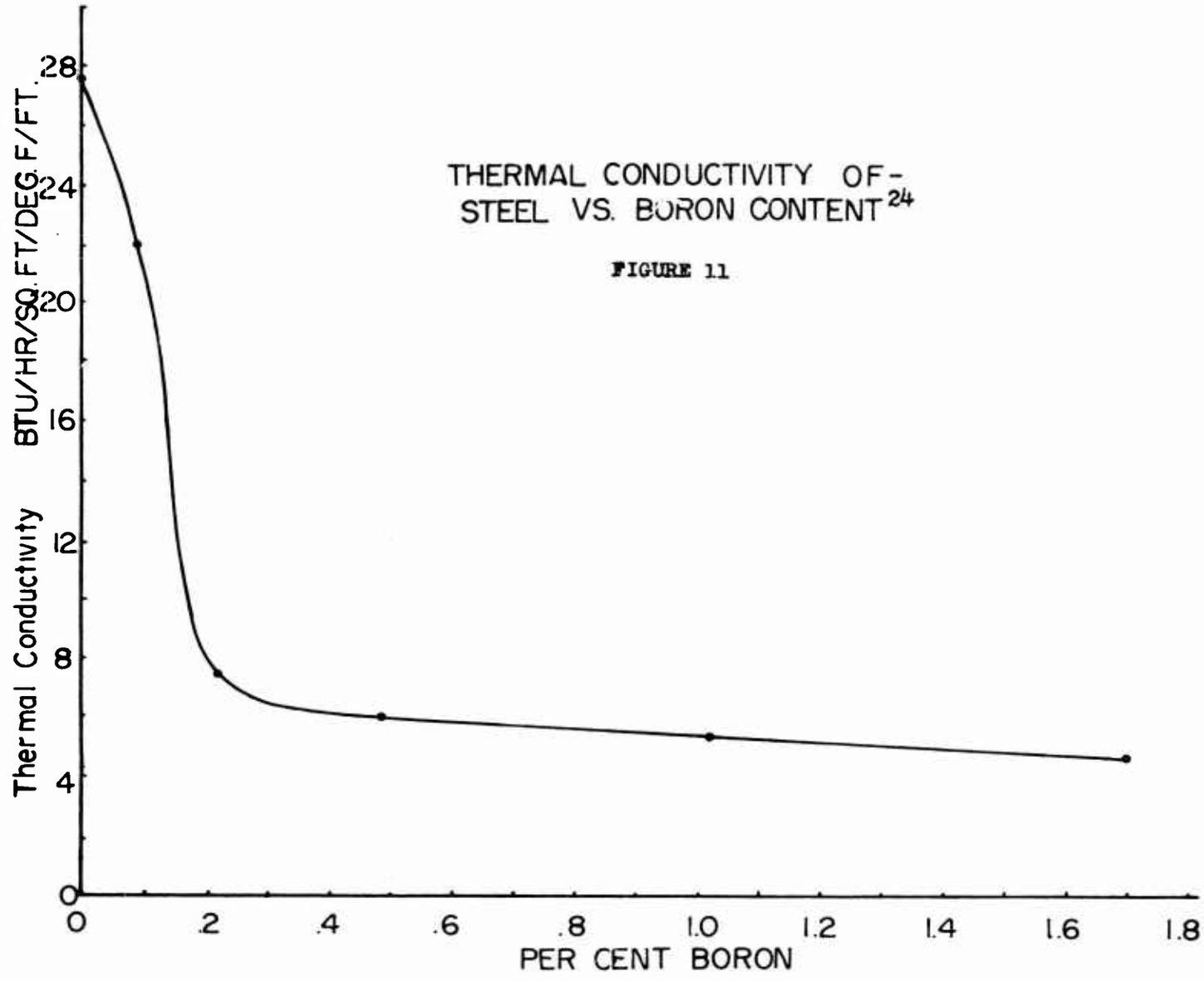

THERMAL CONDUCTIVITY OF-
STEEL VS. BORON CONTENT[24]

FIGURE 11

Several recent reviews of boron steels[39,40] stress that boron must be protected by prior additions of strong deoxidizers sufficient to produce a thoroughly killed steel.

Aluminum is used primarily as the deoxidizing element and since the general consensus of opinion states that boron lowers the coarsening temperature of austenite, some extra aluminum is added to compensate for this effect.

Digges and Reinhart[41] found that the boron effect on hardenability diminished with increasing nitrogen content. This effect was nil in steels containing 0.010% nitrogen. However, if the nitrogen was fixed by additions of titanium or zirconium the hardenability effect is operative.

Imai and Imai[42] state that in general the nitrogen contents of steels prepared in the open hearth, or electric arc and induction furnaces are as follows: (1) open hearth - approximately 0.001 to 0.008%; (2) electric arc and induction furnaces - approximately 0.006 to 0.040%. These authors found that if the nitrogen content in steels treated with boron was greater than 0.008% the boron hardenability effect decreases markedly with increasing amounts of nitrogen. At 0.02% nitrogen the hardenability effect is negligible. In agreement with Digges and Reinhart, the effect is operative if the nitrogen is removed or fixed by titanium or aluminum additions.

A patent[43] was granted to the Carnegie-Illinois Steel Corporation covering the fixation of nitrogen with titanium. This patent states that in steels containing more than 0.006% nitrogen, the titanium addition should be at least five times the amount the nitrogen content which exceeds 0.006%.

Gurry[44] showed by thermodynamic calculations that the deoxidizing power of boron was better than silicon, vanadium or titanium and almost as good as aluminum or zirconium. Derge[45] studied the boron-oxygen equilibrium in liquid iron and the experimental results differed appreciably from Gurry's theoretical calculations. Experimental results show the deoxidizing power of boron is comparable with that of silicon. Chipman[46] reviews the problem of steel deoxidation and remarks that deoxidizers not only remove oxygen from solution but also have a pronounced effect on the activity of oxygen in iron. This author states that the discrepancy between Derge's and Gurry's data may be explained by the effect of boron on the activity of oxygen.

As a means of showing the relative affinity of boron for oxygen and nitrogen in comparison with some of the common alloying elements, the free energies of formation for the oxides and nitrides were calculated from existing data and the results are plotted in Figures 12 and 13. It should be stressed that these results at best are only rough approximations. The free energy equations used and data calculated are given in Tables I-II. Of special interest is the fact that aluminum appears not to be a decisive denitrider in the presence of boron.

2. Type of Boron Additions. Investigations of boron steels have incorporated both additions to the ingot molds and to the ladle. The latter method is more feasible in commercial practice and several investigations[51,52] report that the properties of boron steel produced in this manner were as uniform as boron-free heats. These authors state that in general, the properties of boron steels were not critically dependent upon the kind of ferro-alloy in which boron was added. These heats were prepared in the open hearth.

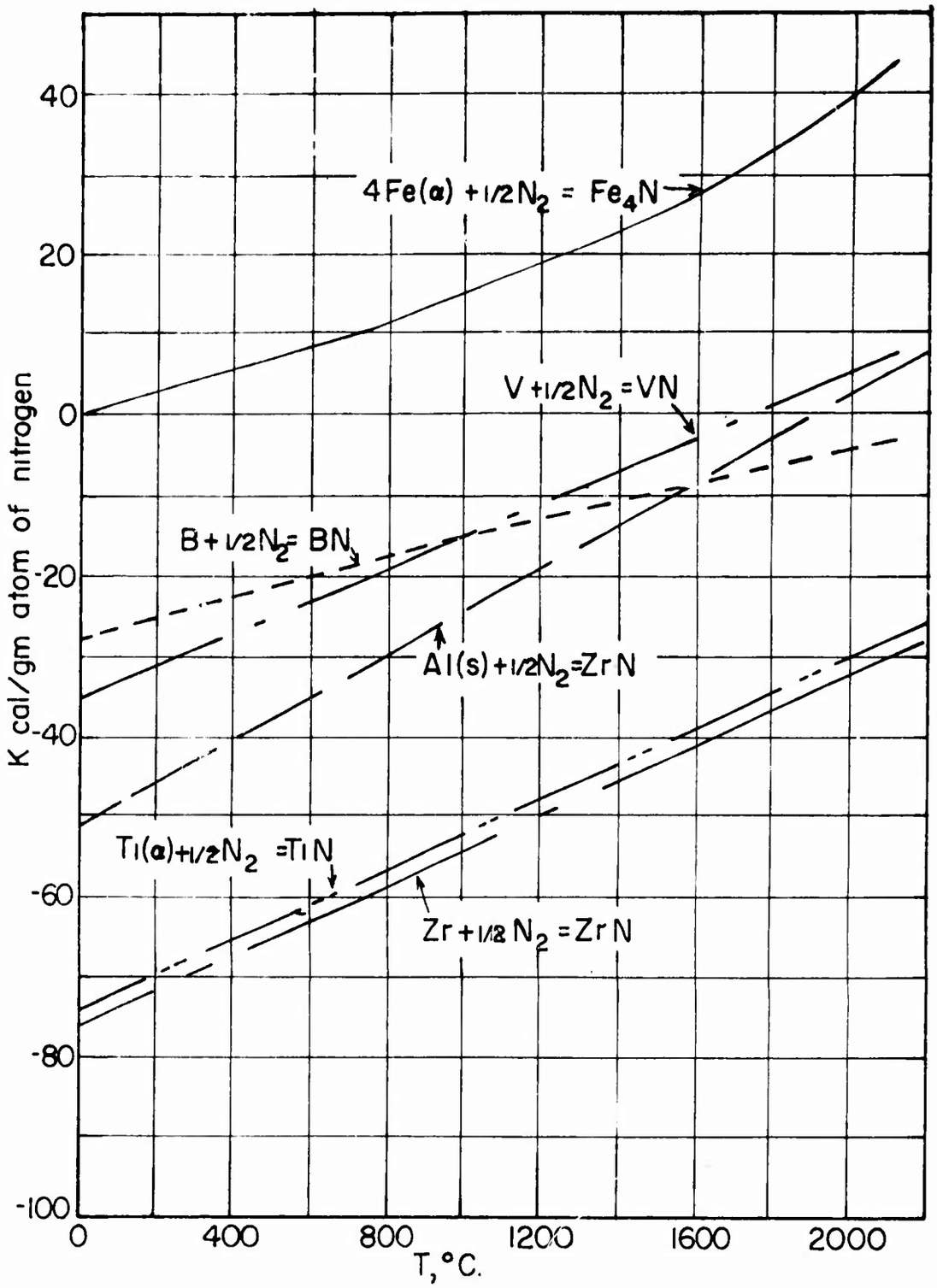

Figure 12. Free Energy of Formation vs. Temperature for Several Nitrides

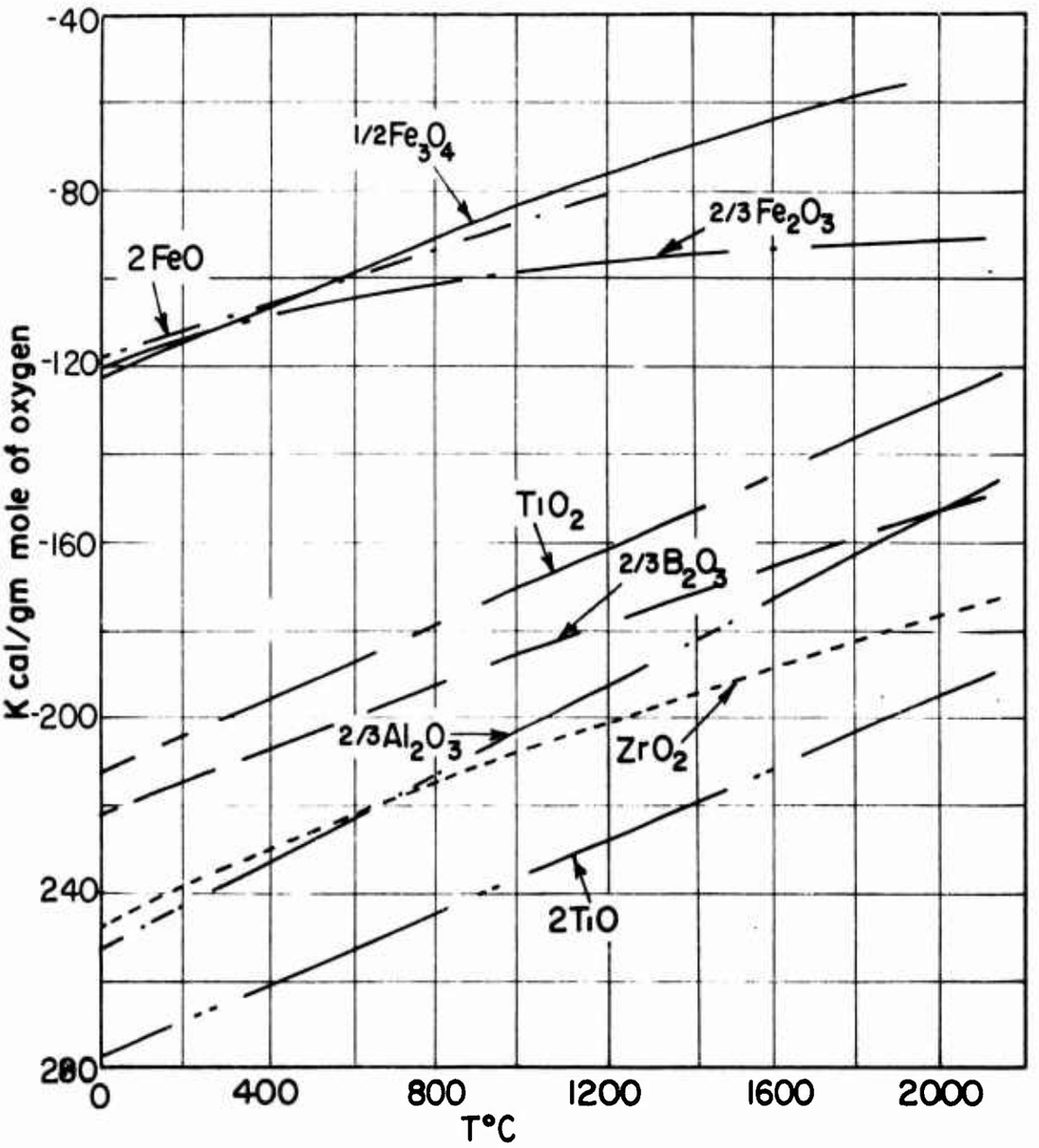

Figure 13. Free Energy of Formation vs. Temperature for Several Oxides

TABLE I

Free Energies of Formation for Several Nitrides as a Function of Temperature

Reaction	Equation	Reference	T°K	ΔF° cal
$Al + 1/2N_2 = AlN$	$\Delta F^\circ = -56{,}950 + 3.45T\log T + 14.61T$	47	298.1	-50,052
			573	-43,126
			873	-35,337
			1173	-27,392
			1473	-19,331
			1773	-11,173
			2073	- 2,941
			2373	+ 5,350
$B + 1/2N_2 = BN$	$\Delta F^\circ = -31{,}200 + 3.62T\log T - 1.55 \times 10^{-3}T^2 + 3.30T$	47	298.1	-31,530
			573	-24,098
			873	-20,806
			1173	-16,490
			1473	-12,809
			1773	- 9,369
			2073	- 6,128
			2373	- 3,098
$4Fe\ (\alpha) + 1/2N_2 = Fe_4N$	$\Delta F^\circ = -3{,}860 - 16.28T\log T + 8.93 \times 10^{-3}T^2 + 53.55T$	47	298.1	890
			573	+ 4,016
			873	+ 7,898
			1173	+12,635
			1473	+18,426
			1773	+25,377
			2073	+33,582
			2373	+43,117

TABLE I (continued)

Reaction	Equation	Reference	T°K	p^{o}_{cal}
$Ti(\alpha) + 1/2N_2 = TiN$	$\Delta F^{o} = -82{,}250 - 8.22T\log T + 1.26 \times 10^{-3}T^{2} + \frac{1.48 \times 10^{-5}}{T} + 47.74T$	50	298.1	-73,473
			573	-67,213
			873	-60,548
			1173	-53,981
			1473	-47,453
			1773	-40,912
			2073	-34,321
			2373	-27,639
$V + 1/2N_2 = VN$	$\Delta F^{o} = -41{,}650 - 1.73T\log T + 26.38T$	47	298.1	-35,060
			573	-29,267
			873	-23,067
			1173	-16,934
			1473	-10,865
			1773	- 4,884
			2073	+ 1,140
			2373	+ 7,094
$Zr + 1/2N_2 = ZrN$	$\Delta F^{o} = -82{,}300 + 22T$	47	298.1	-75,640
			573	-69,694
			873	-63,094
			1173	-56,494
			1473	-49,894
			1773	-43,294
			2073	-36,694
			2373	-30,094

TABLE II

Free Energies of Formation for Several Oxides as a Function of Temperature

Reaction	Equation	Reference	T°K	F°cal
$2Al\ (S) + 3/2O_2 = Al_2O_3$	$\Delta F^\circ = -404{,}500 - 9.58T\log T + 2.18 \times 10^{-3}T^2 + \frac{4.98 \times 10^5}{T} + 257.0 \times T^{1/2} + 99.28T$	50	298.1	-375,677
			573	-355,014
			873	-332,600
			1173	-310,308
			1473	-288,036
			1773	-265,702
			2073	-243,351
			2373	-220,631
$Ti\ (\alpha) + 1/2O_2 = TiO\ (\alpha)$	$\Delta F^\circ = -146{,}600 - 1.95T\log T - 0.227 \times 10^{-3}T^2 + \frac{0.93 \times 10^5}{T} + 85.7T^{1/2} + 26.60T$	50	298.1	-138,339
			573	-132,300
			873	-125,918
			1173	-119,716
			1473	-113,658
			1773	-107,722
			2073	-101,891
			2373	- 94,944
$Ti\ (\alpha) + O_2 = TiO_2$	$\Delta F^\circ = -228{,}320 - 5.74T\log T + 1.125 \times 10^{-3}T^2 + \frac{1{,}795 \times 10^5}{T} + 171.8T^{1/2} + 57.32T$	50	298.1	-211,812
			573	-199,762
			873	-186,869
			1173	-174,177
			1473	-161,533
			1773	-148,901
			2073	-136,257
			2373	-123,513

TABLE II (continued)

Reaction	Equation	Reference	T°K	F°cal
$Zr\ (s) + O_2 = ZrO_2$	$\Delta F^\circ = -259{,}900 + 8.64T\log T - 5.14 \times 10^{-3}T^2 + \frac{0.889 \times 10^5}{T} + 171.4T^{1/2} + 15.79T$	48	298.1	-246,024
			573	-234,627
			873	-222,681
			1173	-211,402
			1473	-200,837
			1773	-191,022
			2073	-181,994
			2373	-173,792
$Fe\ (\alpha) + 1/2O_2 = FeO\ (s)$	$\Delta F^\circ = -65031 - 7.0T\log T + 2.45 \times 10^{-3}T^2 + 85.66T^{1/2} + 33.21T$	48	298.1	-58,602
			573	-54,209
			873	-49,613
			1173	-44,940
			1473	-40,319
			1773	
			2073	
			2373	
$2Fe\ (\alpha) + 1\ 1/2O_2 = Fe_2O_3\ (s)$	$\Delta F^\circ = -195{,}728 - 7.418T\log T - 1.04 \times 10^{-3}T^2 + \frac{2.117 \times 10^5}{T} + 257T^{1/2} + 57.10T$	48	298.1	-179,128
			573	-168,554
			873	-157,889
			1173	-149,959
			1473	-147,869
			1773	-141,489
			2073	-138,711
			2373	-136,797

TABLE II (continued)

Reaction	Equation	Reference	T°K	F°_{cal}
$3Fe(\alpha) + 2O_2 = Fe_3O_4(s)$	$\Delta F^{\circ} = -276{,}405 - 25.89T\log T - 1.012 \times 10^{-3}T^2 + \frac{4.897 \times 10^5}{} + 342.7T^{1/2} + 153.31T$	48	291.1	-242,162
			573	-220,088
			873	-197,578
			1173	-174,852
			1473	-153,961
			1773	-134,563
			2073	-116,419
$2B(s) + 3/2O_2 = B_2O_3(l)$	$\Delta F^{\circ} = -354{,}800 - 28.54T\log T + 2.24 \times 10^{-3}T^2 + 145.6T$	49	298.1	-332,253
			573	-315,738
			873	-299,259
			1173	-282,950
			1473	-268,651
			1773	-254,013
			2073	-239,589
			2373	-225,250

Comstock[53] reports on the effects of eight types of ferro-alloys containing boron to steels prepared in an induction furnace. Results indicate that the complex alloys containing titanium and zirconium were superior to ferro-boron. This is probably due to the fixation of nitrogen which is relatively high in steels prepared in induction furnaces.

Corbett and Williams[54] added boron by additions of either dehydrated borax or fused B_2O_3 glass and found such additions satisfactory.

3. Hardenability. Hardenability may be defined as the lowering of the critical cooling rate to obtain a fully hardened specimen. The prime reason for adding alloying elements to steel is to enhance the hardenability of the steel and thereby the properties of the steel after quench hardening and tempering. The tempered martensite possesses a greater capacity to deform without rupture at any strength level compared to the same strength level obtained by simple cooling or normalizing. The decrease of the critical cooling rate is well known as a displacement of the T-T-T curve to the right.

Steels subjected to hardenability specifications can be classified as (1) shallow hardening, (2) medium hardening, and (3) deep hardening. In general then, hardenability tests are designed primarily for only one classification and these tests are described adequately elsewhere[55].

Grossman[56] presented a method for calculating the hardenability of a steel from its chemical composition which is satisfactory for first approximations. There are many factors which make the determination of hardenability difficult and these are discussed by several authors[57,58,59]. Some of the prominent factors are (1) grain size, (2) concentration gradients of alloying elements, (3) rate of carbon solution in austenite and, (4) non-metallic inclusions.

The influence of the common alloying elements on hardenability has been studied by calculating multiplying factors as proposed by Grossman and some discrepancies are observed[60,61,62].

Literature reporting the effect of small additions of boron on the hardenability of steel is voluminous so that only the pertinent factors will be considered below.

4. Effect of Carbon Content on Boron Hardenability. First the effect of carbon content on the boron hardenability should be considered. Grange and Garvey[63] studied the hardenability of four series of plain carbon steels containing 0.40, 0.52, 0.63, 0.74% carbon. It is shown that the increase in hardenability due to boron decreases with increasing carbon content (see Figure 14). The implication is that boron will not increase the hardenability of hypereutectoid steels. Rahrer and Armstrong[64] investigated steels containing 0.12 to 0.95% carbon and their data confirms the fact that the effect of boron on hardenability becomes negligible at about eutectoid composition. These data indicate that the optimum effect of boron is achieved in steels of 0.40 to 0.60% carbon.

Crafts and Lamont[60] also observed a decrease in boron hardenability with increasing carbon content.

Only one investigation has been reported to date on hypereutectoid steels. Brik, et al[68] studied a steel containing 1.07% carbon and small

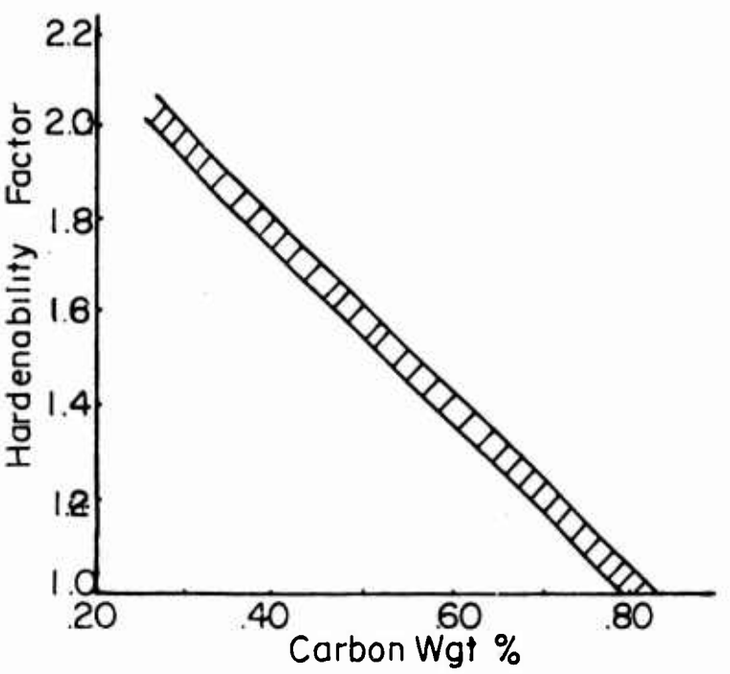

EFFECT OF CARBON CONTENT ON
BORON HARDENABILITY FACTOR [63, 64]

FIGURE 14

additions of boron. Results show that 0.003 to 0.005% boron retarded the transformation of austenite at 400 - 560°C and the hardenability tests parallel this stability.

A recent review[39] states that indications are that optimum effects are obtained when size of the addition introduces from 0.0008 to 0.003% boron into the through-hardening steels. The increase in hardenability appears proportional to the boron content up to about 0.001% boron but beyond this value the hardenability is not affected very much. In the lower carbon steels the optimum effect is obtained at somewhat higher boron contents and the proportional effect appears to continue above 0.003% boron.

It should be noted at this point that confusion may arise in regards to the optimum effect of boron and the correlation between hardenability and boron content due to the so-called effective and ineffective boron. Apparently only the boron atoms in solid solution are effective in increasing the hardenability; thus, any element which tends to tie up boron will decrease this effective amount. Chemical analysis for such small amounts of boron as are utilized in boron steels is obviously difficult and analyzing for only the effective boron appears improbable. Methods used in analyzing for boron are presented in a review of boron literature by Dean and Silkes[65]. Apparently the colorimetric method using quinalizarin is the most satisfactory. Some distinction between effective and ineffective boron may be obtained by analyzing for acid soluble boron as reported by Corbett and Williams[54]. These authors state that soluble and insoluble boron increase linearly as total boron increases with insoluble boron increasing at the greater rate. Further the amount of soluble boron decreases with an increase of carbon content. Such a phenomena might have some bearing on the decrease of the boron effect with increasing carbon content. The amount of soluble boron also decreases with increasing silicon or manganese content.

5. Effect of Other Alloying Elements on Boron Hardenability. The effect of boron on hardenability is apparently enhanced by the addition of other alloying elements such as chromium, manganese and molybdenum. Comstock[53] states that boron exhibits a better effect on manganese steels than on nickel-chromium steels. A similar effect is observed in manganese steels over plain carbon steels[82]. Digges and Reinhart[41] remark that the effectiveness of boron in enhancing the hardenability increased with limiting amounts of manganese, chromium, or molybdenum. Nickel contents up to 0.6% did not have a similar influence. Several authors[62,67] report that boron is more effective in the complex triple alloy type of steel. Udy and Rosenthal[38] observed that increasing molybdenum up to 0.40% enhanced the boron effect.

6. Effect of Boron on the Transformation Points and T-T-T Curves. The effectiveness of boron in enhancing the hardenability of steel is believed to be its action in retarding the rate of nucleation of ferrite while in solid solution in austenite. Thus, its effect on the transformation points and isothermal studies is of primary interest.

Digges, et al[41] state that boron has no significant influence on transformation points and did not affect the Ms temperature. Dilatometer studies of plain carbon steels showed little difference of Ac1, Ac3 or Ar1 but the Ar3 temperature was lowered by 20 to 50°C[66]. This indicates a retardation of the nucleation of proeutectoid ferrite. A notable lowering of the Ar3 was observed in alloy steels containing boron while again no change was noticed in the other transformation points[67].

T-T-T diagrams and corresponding end-quenched hardenability curves have been published by the United States Steel Company for several hypo-eutectoid steels with and without boron additions[69]. A typical curve is reproduced in Figure 15. Boron exhibits a marked retardation on the beginning of ferrite formation and on the formation of upper bainite. Just below Ae_1 boron apparently has little retarding effect on the formation of pearlite and may even accelerate the pearlite transformation. The effect of boron is predominant in the temperature range where fine pearlite and upper bainite are formed. It is of interest to note that the times required for the completion of austenite decomposition are not appreciably affected by boron additions. Thus, in general, the elapsed time between beginning and end of transformation is less for steels containing boron than for non-boron steels.

Brik, et al[68] studied two boron steels containing approximately 0.48% carbon and 1.07% carbon. For the latter steel they report that 0.003-0.005% boron retarded the transformation of austenite at 400 - 560°C and in the 0.48% carbon steel at 320 - 560°C. Further increases in boron accelerated austenite decomposition; at 0.006% boron the austenite transformation was faster than without boron. At higher temperatures (620 - 650°C) even the smallest addition of boron accelerated the rate of austenite transformation. Studies of a 0.30% carbon steel showed a change in the shape of the curve with additions of boron[66]. A decrease in the quantity of proeutectoid ferrite was visible in the structure. The largest effect of boron was observed at the knee and in the upper bainite region.

Potaszkin and Jaspart[67] report that the results of the isothermal studies of Ni-Cr-Mo steels containing boron were similar to the results reported above. Boron shifts the T-T-T curve far to the right. An important retardation of proeutectoid ferrite and a stabilization of austenite in the bainitic region was observed. The nose of the curve is around 600°C but the temperature above which boron accelerates transformation is 650°C. Below this temperature boron retards the decomposition of austenite.

7. Influence of Heat Treating Variables on Boron Hardenability. In general, for any given steel, an increase in austenitizing temperature with accompanying increase in grain size results in increased hardenability. However, boron steels do not behave in this manner. Grange and Garvey[63] studied the effect of austenitizing temperatures upon the hardenability of several boron steel The hardenability was less at austenitizing temperatures of 1093°C (2000°F) than a 816 to 871°C (1500 - 1600°F). Figure 16 shows the results obtained with a 0.25% carbon low alloy steel with and without boron. Full hardenability of samples treated above 982°C could be regained by a second treatment at the optimum temperature of 843°C.

Potaszkin and Jaspart[67] subjected Jominy test specimens of Ni-Cr-Mo steels containing boron to the following treatments: (1) austenitized at 875°C, then water quenched; (2) austenitized at 1100°C, quenched to 875°C, then quenched in water or oil. The higher austenitizing temperature resulted in slightly less hardenability. This decrease in hardenability was accompanied by a characteristic boron constituent at the grain boundaries.

Digges and Reinhart[41] investigated the effect of austenitizing temperature on hardenability for some experimental boron steels containing manganese. In some cases higher austenitizing temperatures were beneficial but detrimental in other cases. The accompanying increase in grain size with increased austenitizing temperatures could explain the increased hardenability for a few steels. However,

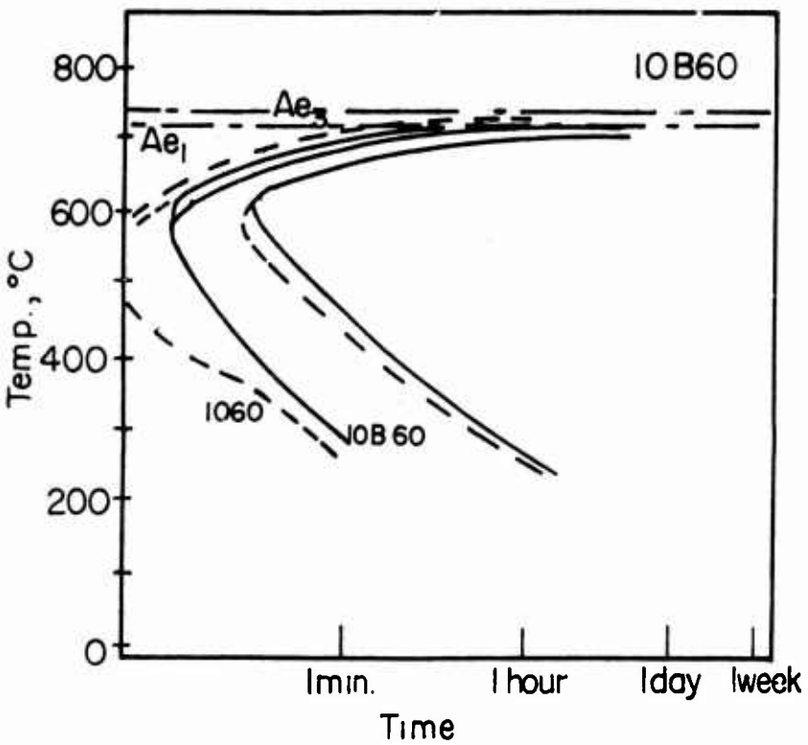

10B60

C-0.63 Mn-0.87 B-0.0018

Austenized at 1500°F., grain size 5-6

T-T-T CURVES FOR 1060 STEEL WITH AND WITHOUT BORON [69]

FIGURE 15

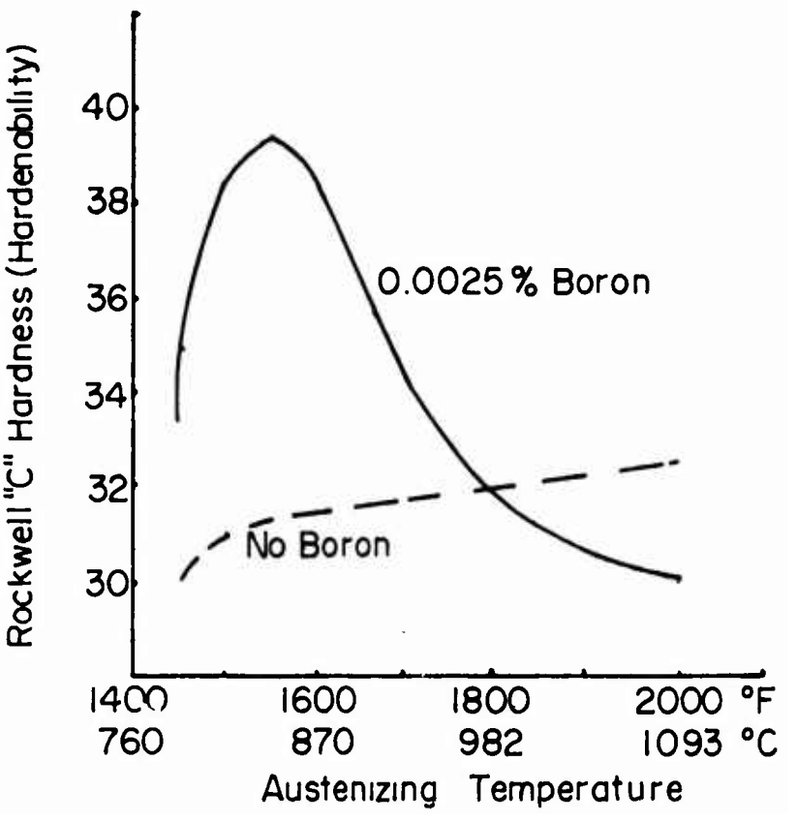

EFFECT OF AUSTENIZING TEMPERATURE ON BORON HARDENABILITY[63]

FIGURE 16

although the grain size was increased in some cases the hardenability decreased. This suggested that some other factor besides grain size is operative which is in agreement with the Grange and Garvey report.

Digges, Irish and Carwile[25] conducted a study of the critical cooling rates as a measure of the hardenability of several high purity steels. The critical cooling rate decreased (hardenability increased) continuously with increased quenching temperatures (from 816 - 1093°C) for non-boron steels containing 0.32% carbon. For 0.50% carbon steels the critical cooling rate was not affected by changes in austenitizing temperatures over a range from 774 to 1093°C. With a 0.70% carbon steel, this rate was approximately constant when the alloy was quenched from temperatures of 774° to 871°C but decreased rapidly with increasing temperatures between 871° to 982°C and less rapidly with further increases up to 1093°C.

For the alloys containing boron, the critical cooling rate decreased continuously with increase in quenching temperatures when the carbon content was 0.47%. With 0.74% carbon a constant rate was observed in the temperature range from 774° to 871°C and a slight decrease in the rate from 871° to 1093°C.

It is stated that the improvement in hardenability of the boron treated alloys was confined primarily to the high range in austenitizing temperatures for the alloys containing approximately 0.5% carbon and to the low range when the carbon content was about 0.7%. The above data were obtained on specimens prepared from homogenized bars and it was shown by the authors that the effect of boron was adversely affected during this operation. Consequently, only tentative conclusions can be made from this work.

Boron does not increase the resistance to softening or tempering as does other alloying elements. Thus, the tempering temperature for boron steels is generally a little lower than required for lean alloy steels.

8. Effect of Boron on the Mechanical Properties. The effect of boron on the engineering factors such as notch toughness, temper brittleness, tensile and yield strengths, etc. are adequately reviewed in numerous recent articles and will not be considered here[70,83]. Boron apparently either exhibits no effect or a detrimental effect on the properties of plain carbon steels in the normalized state. However, it is of interest to consider the results obtained by Bardgelt and Reeve[84]. This paper discusses the results of mechanical tests obtained on several series of low carbon (0.04 to 0.18%) low-alloy steels containing boron in the normalized condition. Additions of 0.003% boron to a mild steel had no effect on the mechanical properties. However, the same amount of boron when added to the same steel with 0.58% molybdenum resulted in an almost doubling the maximum stress and yield stress at the same time retaining good ductility and toughness. The most promising steel contains 0.40% molybdenum, about 0.50% manganese and 0.0015% boron.

D. BORON IN CAST AND MALLEABLE IRON

It is of interest to consider the effect of boron in cast irons as it portrays a reversal in its effect on carbon. Schwartz[71] states that the addition of 1.0% boron to white cast iron rendered the iron unannealable. However, about 0.1% boron increased the rate of graphitization at high temperatures and 0.04% increased it further. Additions of 0.001% considerably accelerated the anneal.

Eckman and Maack[72] obtained patent rights for the small addition of tellurium and boron to cast iron. Tellurium (0.001 - 0.015%) prevents the formation of primary graphite during casting and the boron (0.001 to 0.01%) accelerates graphitization during annealing. Further studies of boron in cast irons are reported by several other authors[73,74,75].

E. MECHANISMS PROPOSED TO EXPLAIN BORON HARDENABILITY

No comprehensive mechanisms have been proposed to explain the effect of boron on hardenability. Boss[78] speculates that this effect can be explained by assuming that even very small amounts of FeO or Fe_2O_3 have a very harmful effect on hardenability. Thus, boron acts as an unusually strong deoxidizer which completely reduces the iron oxide and that a small excess of boron is harmful to hardenability. However, this hypothesis does not appear likely on the basis of the deoxidizing power of boron as determined by either Derge or calculated by Gurry.

Dean and Silkes[65] state that the remarkable effect of boron on hardenability up to 0.0025% and the decrease or reversal effect beyond that point indicates a different mechanism of action than in the case of manganese, chromium, molybdenum and other alloying elements. They state that a dispersion of the boron in austenite is more likely than solution.

Chandler and Bredig[79] propose that boron behaves as a fluxing agent upon the particle size of nitrides of other elements rather than an alloying agent or as a compound former with nitrogen. This is based on the assumption that the nitrides act as nucleating agents in the decomposition of austenite and that the boron behaves as a fluxing agent in reducing the critical size of these nitrides below which they are ineffective. This hypothesis appears to be in direct contradiction to the experimental data reported by Imai and Imai[42]. These latter authors, as reported below, found that boron promotes the precipitation of visible nitride particles.

The investigations conducted by Corbett and Williams[54] show that soluble boron does not increase much beyond the point of maximum hardenability at 0.0025% total boron. These authors believed that both soluble and insoluble boron affect the hardenability but no mechanism was proposed.

Imai and Imai[42] also found a maximum in hardenability with the addition of about 0.003% to a medium carbon steel (0.3%). Further increase in boron showed a sharp decrease in the hardenability effect. These authors isothermally transformed specimens below 400°C and showed that boron accelerated the precipitation of nitrides and suppressed the formation of carbide. Thus, they proposed that the nitride precipitant acts as transformation nuclei for the formation of martensite and also increases the stability of the autenite.

The above authors show that for a steel containing approximately 0.3% carbon and 0.004 to 0.006% nitrogen the maximum hardenability is attained at 0.0027% total boron. The hardenability decreased sharply with increasing boron content up to 0.005% boron. With further increase in boron up to 0.041% the hardenability effect decreases slightly. This was explained by the fact that the precipitation of Fe_2B or a double compound of boron was first observed at the grain boundaries with additions of about 0.0027% boron. Below this value evidently the boron content is below the saturation point. Above 0.0027% boron, the amount of this characteristic precipitate increased markedly. Therefore,

on quenching these precipitates act as nuclei for the formation of ferrite and thus decrease the relative hardenability. Hence, the critical amount of boron for the steel studied should be lower than 0.0027%.

Grange and Garvey[63] found the best correlation between hardenability and the quantity of the characteristic boron constituent at austenite grain boundaries which is obtained by a special heat treatment. The authors state that if the boron content is less than 0.0004% the compound does not form. Grange and Garvey propose that the boron atoms are preferentially located at the austenite grain boundaries just prior to transformation and in some manner inhibit grain boundary nucleation. It is further assumed that this enrichment of boron atoms at the grain boundaries may result in some precipitation of a boron compound but that only that boron remaining in solid solution is effective in retarding nucleation of ferrite.

It is of interest to note that these authors state that the effect of austenitizing temperatures on boron hardenability may be explained due to an unfavorable distribution of boron in austenite. At relatively low austenitizing temperatures undissolved particles remain which might contain some carbon and boron atoms. The decrease in boron hardenability of the higher carbon steels may be due to insufficient austenitizing temperatures for the solution of such particles. It is further stated, however, that higher austenitizing temperatures may lead to unfavorable distribution of boron and result in decreased hardenability.

This so-called unfavorable distribution may be explained by the grain boundary mechanism proposed by Spretnak and Speiser[80]. Assuming that boron in iron exhibits a positive deviation from Raoult's Law it is shown that such solute elements are preferentially absorbed at grain boundaries and this enrichment increases with increasing temperatures.

Thus, when the absorption of boron exceeds the solubility limit at a given temperature a boron compound may precipitate. Then upon quenching from this temperature the precipitate act as nucleating agents for the decomposition of austenite and thus reduce the relative hardenability.

Corson[81] suggested that boron increases hardenability by acting as a scavenger for some deleterious agent, such as perhaps nitrogen.

Digges, Irish and Carwile[25] state that only the boron in solid solution is effective in enhancing hardenability and that it decreases the rate of nucleation of ferrite and carbide.

II. THE MECHANISM OF THE BORON EFFECT

F. INTRODUCTION

The primary objective of this research project is the clarification of the mechanism of the boron hardenability effect in heat treatable steels. Accordingly, one of the results of this correlated review of the pertinent information on boron should be a working hypothesis based on a critical evaluation of data on decomposition of austenite in general and on data relating to the transformations in boron treated steels. Such a hypothesis would serve as a basis of planning and designing of critical experiments on the boron effect.

G. SPECIFIC EFFECTS OF BORON

It is logical first to consider the specific effects of boron in hardenable steels. The principal effect, of course, is a significant increase in hardenability with as little as 0.0005% boron; i.e., the critical cooling rate is decreased by boron. The effectiveness of boron is inversely proportional to the carbon content and is essentially nil at eutectoid composition. There is some divergence in opinion as to whether or not boron exerts an effect in hyper-eutectoid steels. However, the best information indicates that the boron effect is indeed restricted to hypo-eutectoid steels. This point should be established definitely by experimentation since it is important fundamentally. Accepting the above tentative conclusion, one can state consequently that the effectiveness of boron is inversely proportional to the amount of pro-eutectoid ferrite characteristic of the carbon content.

Examination of transformation diagrams of boron steels leads to some general observations:[85]

1. Boron effectively delays the start of transformation in the temperature range from A_{e3} to roughly the middle of the bainite range.

2. Boron likewise delays the beginning of the transformation to pearlite following the formation of pro-eutectoid ferrite.

3. Boron has essentially no effect on the time for completion of the transformation. A single exception can be cited for the upper bainite region just under the nose of the curve. This region will be discussed in a subsequent section. It appears that this effect is a result of a change in the basic transformation mechanism induced by boron in this temperature range.

From the viewpoint of engineering properties, it may be said that in general boron imparts only a hardenability effect without a change in the inherent combination of mechanical properties when quenched out to martensite. Care must be exercised in comparing properties always to take into account the base composition of the steels. There are some reports that boron reduces impact properties, but this point needs clarification.

H. GRAIN BOUNDARY EFFECTS

There have been at times suggestions that boron may form a film entirely around the austenite grain or that a film of the compound Fe_2B may similarly form and be the mechanism of the hardenability effect. In this connection, it is of interest to examine some of the ramifications of the concentration range of boron employed, namely 0.0005 to 0.003 per cent in a grain size range of ASTM Grain Size No. 1 through 10.

The ratio of the iron to boron atoms and the number of unit cells of gamma iron per boron atom are listed in the following table:

Weight % B	Ratio of iron to boron atoms	No. of Fe unit cells per boron atom
0.0005	3.87×10^4	9.97×10^3
0.0010	1.93×10^4	4.83×10^3
0.0015	1.29×10^4	3.22×10^3
0.0020	9.68×10^3	2.42×10^3
0.0025	7.75×10^3	1.94×10^3
0.0030	6.65×10^3	1.66×10^3

It is of interest to note that even at the highest concentration, there are 1600 unit cells of iron per boron atom, assuming, of course, a uniform distribution of boron.

The diameter, area, volume, and number of unit cells for the various grain sizes are listed in Table III, along with the total number of boron atoms per grain as a function of grain size and composition. Despite the low concentrations, the total number of boron atoms per grain is of an appreciable order of magnitude.

The possibility of forming a complete boron film on the grain boundary is first considered. For the purpose of this calculation, the extreme case of 100% adsorption of boron to the grain boundary is assumed. (In reality, this is highly improbable because of the very limited solid solubility of boron in iron.) Boron prefers to crystallize in equilaterial hexagonal sheets;[16] the selected value for the length of a side is 1.80 Å. A simple calculation shows that two boron atoms cover an area of $8.4 \times 10^{-16} cm^2$. By using the surface area of the grain and the total number of boron atoms per grain, one can test the possibility of such a boron network for various grain sizes and concentrations. At 0.0005% B, such a film is possible for grain sizes up to Grain Size No. 6; at 0.001% B, the film is possible up to grain size No. 9; at 0.015% B, the film is possible up to grain size No. 10. At higher concentrations, the boron film is possible for all the grain sizes considered. Again, it should be emphasized that this assumes 100% adsorption of boron. Such an event is highly improbable, since on reaching the limit of solubility in the grain boundary area, further adsorption could occur only through the precipitation of Fe_2B from solid solution. If such a film does form, it would be expected that it would have a pronounced effect on the interfacial tension.

TABLE III

ASTM Grain Size No.	Diameter in Microns	Data on ASTM Grain Sizes: Surface Area of Grain cm^2	Volume of Grain cm^3	Number of Unit Cells per Grain	Number of Cube Faces on Surface of Grain
1	280	2.57×10^{-3}	1.22×10^{-5}	2.55×10^{17}	1.94×10^{12}
2	200	1.28×10^{-3}	4.32×10^{-6}	8.98×10^{16}	9.70×10^{11}
3	150	6.44×10^{-4}	1.54×10^{-6}	3.20×10^{16}	4.87×10^{11}
4	100	3.21×10^{-4}	5.43×10^{-7}	1.13×10^{16}	2.43×10^{11}
5	70	1.61×10^{-4}	1.92×10^{-7}	3.99×10^{15}	1.21×10^{11}
6	50	8.04×10^{-5}	6.78×10^{-8}	1.41×10^{15}	6.08×10^{10}
7	35	4.02×10^{-5}	2.39×10^{-8}	4.99×10^{14}	3.04×10^{10}
8	24	2.03×10^{-5}	3.58×10^{-9}	1.79×10^{14}	1.53×10^{10}
9	18	1.02×10^{-5}	3.05×10^{-9}	6.36×10^{13}	7.70×10^{9}
10	12	4.52×10^{-6}	$9.05 \times$ [illegible]	1.88×10^{13}	3.42×10^{9}

ASTM Grain Size No.	Number of Boron Atoms per Grain: 0.0005	0.0010	0.0015	0.0020	0.0025	0.0030
1	2.63×10^{13}	5.27×10^{13}	7.90×10^{13}	1.05×10^{14}	1.32×10^{14}	1.58×10^{14}
2	9.29×10^{12}	1.85×10^{13}	2.79×10^{13}	3.72×10^{13}	4.64×10^{13}	5.58×10^{13}
3	3.31×10^{12}	6.62×10^{12}	9.93×10^{12}	1.32×10^{13}	1.66×10^{13}	1.99×10^{13}
4	1.17×10^{12}	2.34×10^{12}	3.50×10^{12}	4.67×10^{12}	5.84×10^{12}	7.01×10^{12}
5	4.13×10^{11}	8.27×10^{11}	1.24×10^{12}	1.65×10^{12}	2.07×10^{12}	2.48×10^{12}
6	1.46×10^{11}	2.92×10^{11}	4.38×10^{11}	5.84×10^{11}	7.30×10^{12}	8.76×10^{11}
7	5.17×10^{10}	1.03×10^{11}	1.55×10^{11}	2.06×10^{11}	2.58×10^{11}	3.10×10^{11}
8	1.85×10^{10}	3.69×10^{10}	5.54×10^{10}	7.39×10^{10}	9.24×10^{10}	1.11×10^{11}
9	6.58×10^{9}	1.32×10^{10}	1.97×10^{10}	2.63×10^{10}	3.29×10^{10}	3.95×10^{10}
10	1.95×10^{9}	3.89×10^{9}	5.84×10^{9}	7.79×10^{9}	9.74×10^{9}	1.17×10^{10}

It can be next assumed that as the limit of solid solubility of boron at the grain boundary is exceeded through the adsorption effect, some boron would be precipitated as Fe_2B, allowing subsequent adsorption to continue. It could be argued that such a process could be continued until all the boron atoms have been precipitated at the grain boundary, forming a film of Fe_2B on the grain surface. Calculations were made on the possibility of forming a single layer of Fe_2B on various grains at several concentrations of boron. Such a film is possible up to grain size No. 7 for 0.0005% B, up to grain size No. 9 for 0.0010% B, and up to grain size No. 10 for 0.0015% B. The Fe_2B film is possible for all grain sizes considered in the concentration range of 0.0020 to 0.0030% B.

Although these calculations show that an iron boride film is possible in some cases from a concentration viewpoint, certain aspects of the boron hardenability effect lead to the conclusion that such a film does not form in ordinary heat treating procedures and that such a film is not responsible for the hardenability effect. First of all, it is well agreed that the magnitude of the hardenability effect is dependent upon the amount of boron in solid solution. Secondly, from the behavior of the metallographic test for boron, it appears that boron does not readily precipitate out at temperature in the austenite range. The initial step in the metallographic test is to austenitize at a very high temperature. It is presumed that this step builds up the boron content in solid solution at the vicinity of the grain boundaries by adsorption effects. The specimen is then quenched rapidly to a sub-critical temperature to develop a ferrite rim. It is observed that the boron precipitate is formed with time in the ferrite rim from the solid solution which became supersaturated as a result of the temperature change; the precipitate does not form at the austenitizing temperature. A third factor is the observation that the boron is more effective with faster cooling rates through the austenite range. At intermediate cooling rates, it would be expected that the precipitation of Fe_2B would be promoted, and slow rates would allow boron in the grain boundaries to diffuse back into the interior of the grain on reducing the temperature.

Although it is very unlikely that either a boron film or an iron boride film is the underlying boron hardenability mechanism, the possibility of adsorption effects involving boron in solid solution in austenite appears to be of primary importance in explaining some aspects of the boron hardenability effect. By adsorption it is meant the enrichment or depletion of a solute atom in the vicinity of the grain boundary without precipitation as a result of surface tension effects. Positive adsorption signifies an enrichment of the grain boundary and negative adsorption a depletion of the solute at the grain boundary. The underlying principle of adsorption effects is the minimizing of the total free energy of the system by minimizing the surface energy. A solute species with surface tension lower than the solvent species would tend to concentrate at the grain boundary and in the reverse case, in the interior of the grain. Effects of this type have been reported previously in the literature for aluminum-copper alloys[86] and for zinc-copper alloys.[87]

Spretnak and Speiser[80] have examined the thermodynamic conditions leading to adsorption effects. The following basic equation is given:

$$N_2\left(\frac{\Gamma_2^\sigma}{N_2} - \frac{\Gamma_1^\sigma}{N_1}\right) = -\frac{\partial\gamma}{RT\,\partial\ln(f_2 N_2)} \qquad (1)$$

where

N_1, N_2 = mole fraction of solvent and solute respectively in the homogeneous phase

Γ^σ = surface excess

γ = surface tension

R = gas constant

T = absolute temperature

f_2 = activity of solute in the homogeneous phase.

Positive adsorption occurs when $\frac{\Gamma_2^\sigma}{N_2} > \frac{\Gamma_1^\sigma}{N_1}$

and negative adsorption occurs when $\frac{\Gamma_2^\sigma}{N_2} < \frac{\Gamma_1^\sigma}{N_1}$

Examination of Equation 1 shows that if the surface tension decreases as the mole fraction of solute in the homogeneous phase is increased, an excess of solute will be present in the surface phase, whereas if the surface tension increases, there will be a deficiency of the solute in the interface.

It was further demonstrated that the temperature coefficient of adsorption is positive if the temperature coefficient of the surface tension is negative. Also, the positive adsorption at the interface is greater, the greater the positive deviation of the homogeneous phase from Raoult's law. Phase separation can be considered as a case of extreme physical adsorption at the interface. Carbon has been found to exhibit a marked positive deviation in austenite.[88] Since one would expect the surface tension of solid iron to decrease with temperature, carbon will concentrate increasingly at the austenite grain boundaries with rising temperature and will diffuse away from the grain boundary with decreasing temperature. Formation of proeutectoid ferrite can be considered to be a case of extreme negative adsorption on reduction of temperature into the sub-critical range.

There are no direct data as yet on the activity of boron in austenite. However, certain aspects of the hardenability effect strongly point to the occurrence of significant adsorption effects of boron in gamma iron. Important to consider in this respect is the metallographic test for boron.[63] Briefly, the process is to austenitize the specimen at a very high temperature, quench rapidly to a sub-critical temperature at which a ferrite rim can form, and finally a quench to room temperature in order to convert the

remaining austenite to martensite. The boron precipitate occurs as fine dots in the ferrite rim. It is evident that the solid solution at the grain boundary brought down from the high temperature must become a super saturated solid solution at the reaction temperature; the concentration at the high temperature must be more than the solubility at the ferrite reaction temperature. This enrichment can be explained by increasing positive adsorption of boron with increasing austenitizing temperature. It is also necessary to cool rapidly through the austenite range to prevent diffusion of boron from the grain boundary to the interior of the grain as discussed previously for the case of carbon. In agreement with this explanation, it is observed that the higher the boron content, the lower is the austenitizing temperature required to form the boron precipitate.

It is of interest to consider the order of magnitude of the adsorption effects. For the purpose of these calculations, ASTM grain size No. 7 is selected and the solubility of boron in austenite is estimated to be 0.0015% at the sub-critical reaction temperatures; the enriched grain boundary area will be assumed to be 50 Å in thickness. For an initial boron content of 0.0005%, 0.085% adsorption will be required to double the boron content in the grain boundary volume. This means that 0.085% of the boron atoms in the interior of the grain must diffuse to the grain boundary. To obtain 0.0015% B (the assumed saturation) at the grain boundary, 0.17% adsorption is required. In the case of initial content of 0.001% B, 0.043% adsorption would be required for saturation. It is evident that the magnitude of adsorption effects to enrich the grain boundary volume is of relatively small order.

In this connection, it is of interest to note that 0.0004% B is reported to be the lower limit for obtaining the boron precipitate.[65] Using again the assumed solubility of 0.0015% B at the sub-critical reaction temperatures, it is evident that employing the maximum austenitizing temperatures, the grain boundary can be enriched by adsorption to a maximum of somewhat over triple the average concentration.

I. CLUSTERING EFFECTS IN AUSTENITE

There are two basic steps in the formation of pro-eutectoid ferrite from austenite in steels. The first step is the depletion of carbon content in a region to a concentration corresponding to the solubility of carbon in alpha iron. The second step, of course, is the transformation of iron from the face centered lattice to the body centered lattice. The sequence of steps might be argued, namely that the transformation precedes the partitioning of carbon. However, the latter sequence is not likely as will be discussed in detail in the section on the mechanism of transformation of austenite to ferrite.

Thus, an important step in the formation of pro-eutectoid ferrite is the occurrence of embryo of austenite with very low carbon contents. A schematic diagram is given in Figure 17 for distributions of embryo concentrations in a hypo-eutectoid steel for the cases of ideal solution

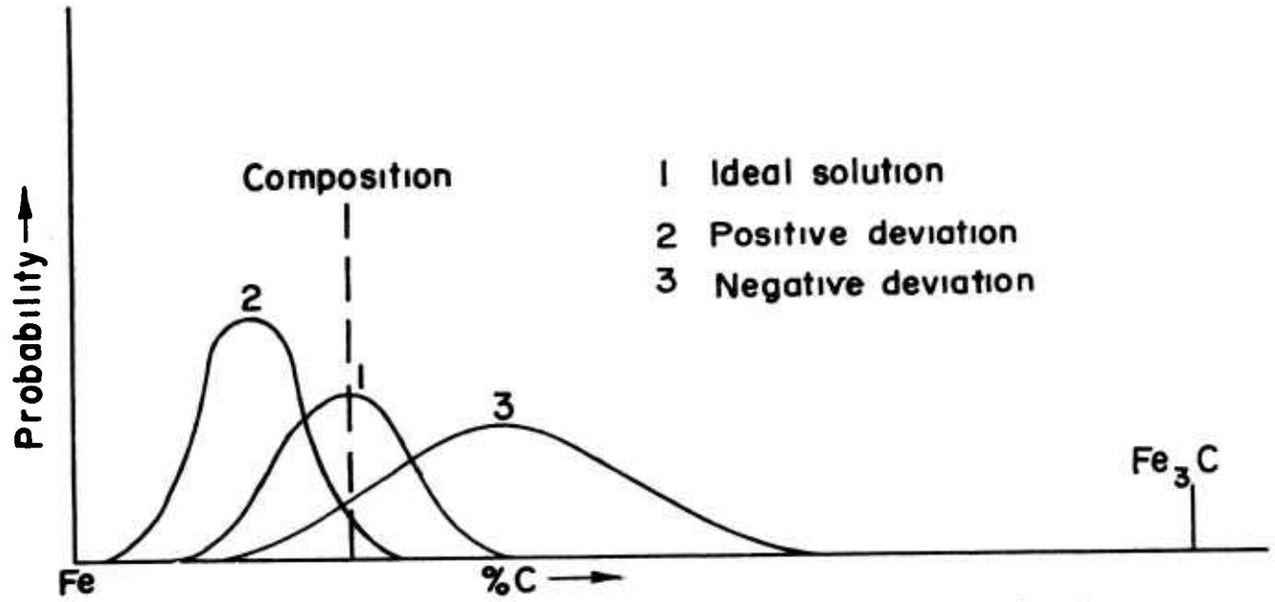

Figure 17. Schematic Diagram for Distribution of Embryo Concentrations for Ideal Solution Behavior, Positive Deviation, and Negative Deviation from Ideality

behavior, positive deviation from Raoult's law, and for negative deviation from Raoult's law. The diagram is a method of illustrating the concentration fluctuations in austenite. For the case of the ideal solution, the distribution is symmetrical about the average composition as the central value. In this case, the probability of obtaining compositions corresponding to either ferrite or cementite is low. If carbon exhibits a positive deviation in austenite (as it actually does), then the distribution of compositions is given by Curve No. 2. Now the probability of obtaining composition of clusters corresponding to ferrite is relatively high and that for cementite is low. If a negative deviation is exhibited, the distribution curve is shifted to higher carbon contents increasing the probability of nucleating cementite (Curve No. 3). In a hypo-eutectoid steel, the nucleation of cementite leading to pearlite formation results from a continuous enrichment of the austenite ahead of the ferrite, pushing the distribution curve continuously to the right until cementite forms.

Thus from the viewpoint of composition requirements, the ferrite reaction might be influenced by (a) a diminished rate of diffusion of carbon, and (b) a change from a positive deviation from Raoult's law of carbon in austenite to a negative deviation (or at least a reduced positive deviation). Before evaluating these two possibilities, it is necessary to examine the properties of the interstitial holes in gamma iron.

Figure 18 illustrates the interstitial holes in the face centered cubic lattice in which the carbon and boron atoms are located. An interstitial hole is surrounded by six nearest neighbors of iron atoms at a distance of 0.5 a_o and by 12 next to nearest neighbors of interstitial holds at a distance of 0.707 a_o. Thus, an interstitial atom is in an environment essentially of iron because of the geometry of the lattice. The interaction energy falls off as $1/r^n$ where r is the distance and n is a number from 6 - 10. Assuming n=6, the interaction between an interstitial solute atom and a nearest neighbor interstitial atom is about one tenth that of the interaction with iron. The argument against important interaction between carbon and boron is strengthened if one considers the concentrations. A composition of 0.40% C and 0.001% B is assumed with a uniform distribution of solute atoms. The mole fractions are the following:

$$N_C = 0.018317$$

$$N_B = 0.0000508$$

$$N_{FC} = 0.98111$$

Since the number of holes per lattice is the same as the number of iron atoms, the mole fraction of the holes is equal to the mole fraction of iron. At this concentration, one out of 55 holes is filled with carbon and one out of 19,300 holes is filled with boron. Consider next a given carbon atom. It is surrounded by six nearest neighbors of iron and twelve next to nearest interstitial holes. The probability of any given hole being filled with boron is 0.00005. The probability that this carbon atom will have a next to nearest boron neighbor is 0.0006, or six chances in ten thousand. Thus, from these arguments it is very unlikely that there is any important chemical

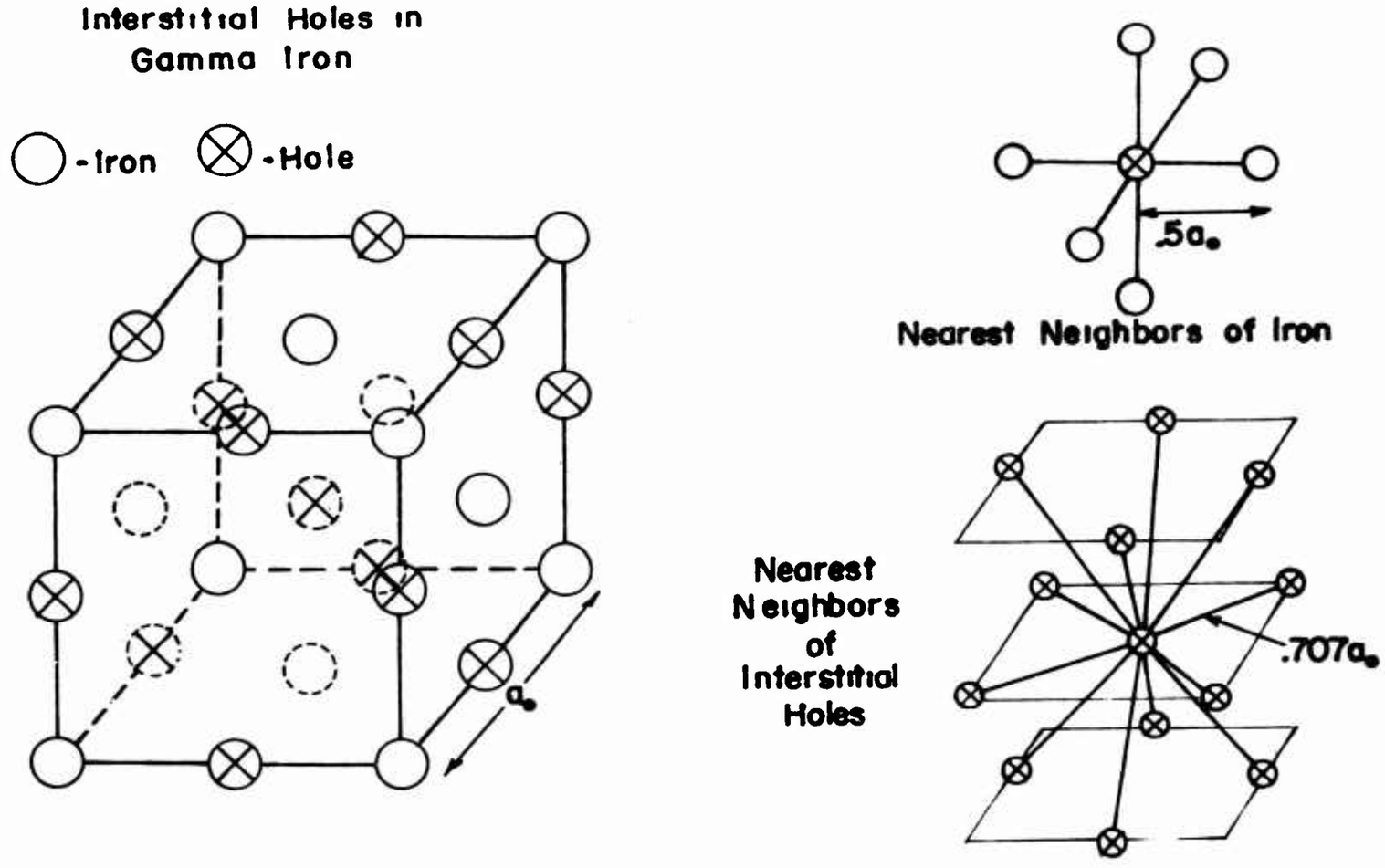

Figure 18. Interstitial Holes in Face Centered Cubic Lattice. The Nearest Neighbors to an Interstitial Hole are Iron Atoms, and the next to Nearest Neighbors are Holes

interaction between carbon and boron atoms in gamma iron. Each would be expected to behave as they do in binary solid solutions in gamma iron.

Because of this likely lack of interaction between boron and carbon, it is presumed that boron does not have an important effect on the diffusivity of carbon in austenite. Molybdenum, a strong carbide former but a substitutional alloying element, was found to have but a minor effect on diffusivity of carbon compared to the hardenability effect.[36] For an 0.80% C, 0.80% Mo steel, the time of the pearlite formation was increased by a factor of 28,000 as compared to a plain carbon steel but the diffusivity of carbon was decreased by a factor of only 5. Despite these arguments, the effect of boron on the diffusivity of carbon in austenite probably should be checked experimentally. The probability of boron causing carbon to show a negative deviation in solid solution can be considered to be nil.

Out of these considerations comes the question as to what effect increasing the carbon content will have on the solubility of boron in gamma iron. As more carbon atoms are introduced into the lattice, more strain energy arises. This in general would be expected to reduce the ability of boron to fit into the interstitial sites and thus decrease the solubility. The effect of carbon content on the solubility of boron in austenite should be checked. If such an effect is observed, it could explain in part the decreased effectiveness of boron with increasing carbon content.

J. TRANSFORMATION KINETICS IN A BORON STEEL

Gudtsov and Nazarova[89] have studied in detail the kinetics of decomposition of austenite in a base composition steel with and without boron. The steel was a manganese-silicon-chromium steel of the following composition:

C	Mn	Cr	Si	B
0.30	1.20	1.30	1.30	0.0017

The progress of isothermal transformation was followed by magnetometric methods.

The fraction transformed is plotted against the logarithm of elapsed time in seconds in Figure 19 for 650°C and 600°C for the base composition and for the base composition with 0.0017% boron. The temperature of 650°C corresponds to the pearlite knee and 600°C is in the upper bainite region. Both curves at 650°C and the curve for the boron steel at 600°C are typical sigmoid curves of the type expected for isothermal nucleation and growth reactions. The base composition steel gives a highly distorted sigmoid curve at 600°C. None of the four curves are parallel to a computed curve in which the rate of nucleation and the rate of growth remain constant. Thus, it is clear that either or both of these factors vary during the transformation. At both temperatures, it is apparent that boron delays the initiation of the transformation, but has little effect on the time for completion of the transformation.

The basic equation for an isothermal nucleation and growth reaction is given by Johnson and Mehl[90] as

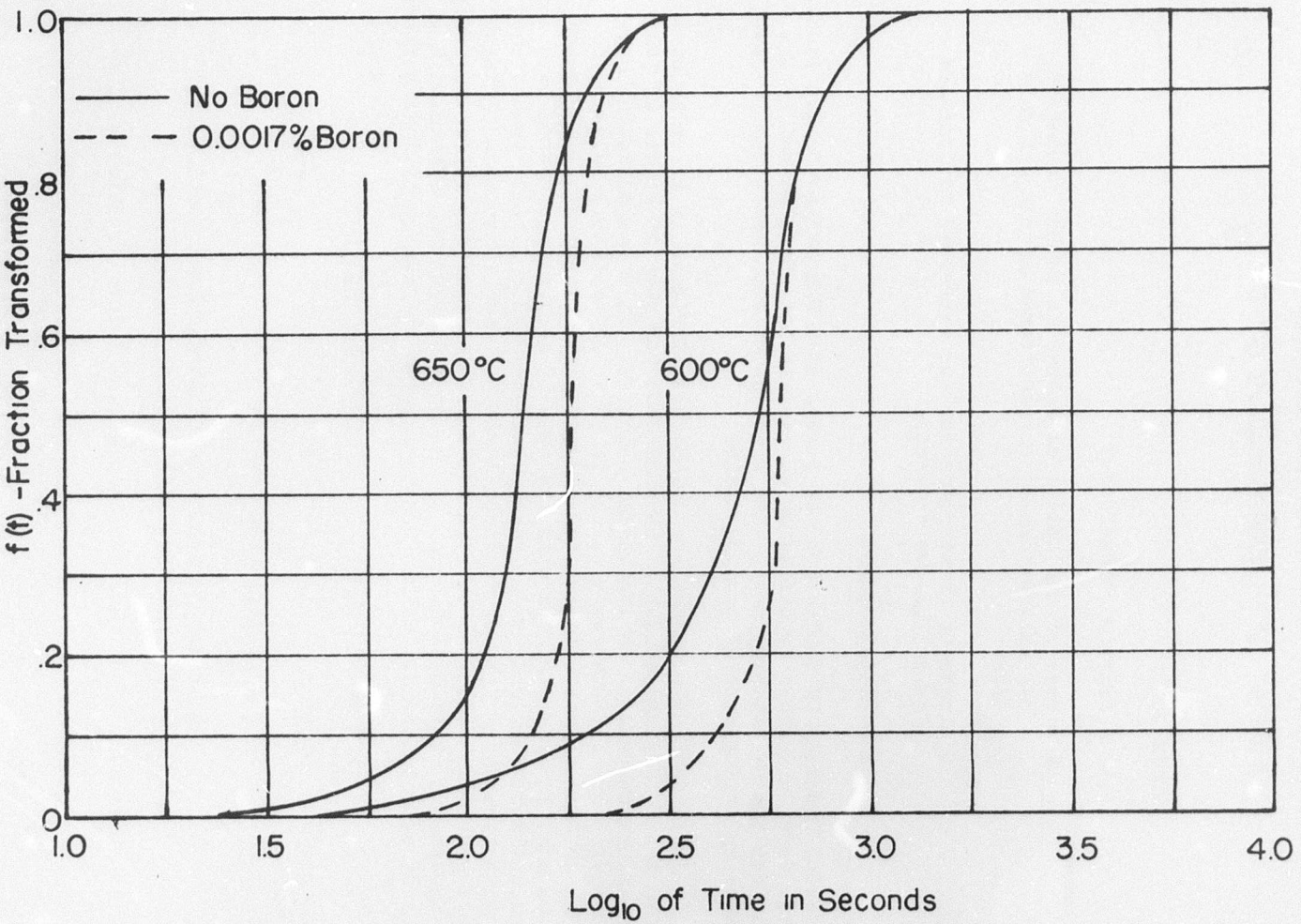

Figure 19. Isothermal Transformation Kinetics of a Mn-Cr-Si Steel with and without Boron at 650°C and 600°C

$$f(t) = 1 - \exp\left\{-\frac{\pi}{3} N G^3 t^4\right\} \qquad (2)$$

where

f(t) = fraction transformed

N = rate of nucleation expressed as number of nuclei per unit volume of untransformed matrix per unit time

G = rate of growth of a nucleus expressed as increase in radius per unit time

t = elapsed time.

A reaction proceeds by nucleation and growth if a thermodynamically stable nucleus forms and grows by diffusion across the interface formed by the stable and the metastable phase. The kinetics of such reactions is complicated by impingement of growing nuclei.

It is desirable to analyze the curves of Figure 19 in terms of N and G. A simplifying assumption is made that the rate of growth of pearlite remains constant in an isothermal reaction. This assumption is harmonious with experimental work on pearlite.[91] A reasonable value of $G = 3 \times 10^{-5}$ cm/sec was selected for the analysis. Examination of Equation 2 shows that in order to determine the rate of nucleation, a trial and error method would be required. Also since G was assumed constant, then N must vary with time and a form of Equation 2 must be used in which a variation in N is provided. In order to circumvent such a laborious procedure, Johnson[92] has suggested a rapid method to obtain an equation for the change of N with time. He selects the following form to express the change of N with time:

$$N = N_o t^x \qquad (3)$$

where

t = elapsed time

N_o, x are constants for a particular reaction temperature

Assuming a constant G and introducing Equation 3 into Equation 2, the general nucleation equation becomes

$$f(t) = 1 - \exp\left[-\frac{8\pi G^3 N_o t^{(4+x)}}{(x+1)(x+2)(x+3)(x+4)}\right] \qquad (4)$$

Transposing and taking logarithms twice yields

$$\log \ln\left[\frac{1}{1 - f(t)}\right] = \log \frac{8\pi G^3 N_o}{(x+1)(x+2)(x+3)(x+4)} + (4+x) \log t \qquad (5)$$

A straight line results if the logarithm of the natural logarithm of $\frac{1}{1-f(t)}$ is plotted against the logarithm of time. The slope of this line is $(4 + x)$. The value of No is obtained from the lateral displacement of the line. Thus Equation 3 can be evaluated.

Such plots of the data for 650°C and 600°C temperatures are presented in Figure 20. At 650°C, the steel without boron interestingly shows two straight line sections. At this temperature, the data for the boron containing steel yield but one straight line. However, at 600°C in the upper bainite region, one straight line is obtained for both steels; the line for the boron free steel is nearly parallel to the initial portion of the same steel at 650°C, whereas the line for the boron steel at 600°C is more nearly parallel to the second part of the curve.

The above analysis for No and x was applied to the data for 650°C. It is of interest that x has a negative value for the initial line for the boron free steel. This is interpreted as a breakdown of the analysis of the initial stage of transformation in terms of nucleation and growth of impinging spheres. A negative value of x gives a continuously decreasing N, contrary to all data on previous measurements for decomposition of austenite which show either constant N or increasing N with time. Since this is a 0.30% carbon steel, the initial part of the curve very likely describes the progress of the formation of pro-eutectoid ferrite. The second part of the curve then describes the formation of pearlite. Consequently, boron at this temperature essentially completely suppresses the formation of pro-eutectoid ferrite since only one straight line is obtained. The equations for rate of nucleation of pearlite as a function of time is

$$N = 0.067\ t^{0.14} \tag{6}$$

for the boron free curve, and

$$N = 6.489\ t^{3.31} \tag{7}$$

for the boron containing steel. These curves are plotted in Figure 21. Thus, the rate of nucleation of pearlite is accelerated in the boron steel, accounting for the comparable times for completion of the transformation despite the delay in the start of transformation caused by boron. Boron thus has a potent effect in suppressing the formation of ferrite. This in turn suppresses the formation of pearlite since it does not enrich the austenite in carbon ahead of the ferrite phase, making the probability of nucleating Fe_3C small. Once started, the pearlite formation is actually faster in the boron steel, perhaps because of the increased incubation period. At the nose of the curve, boron serves only to suppress the formation of ferrite.

At 600°C, the curve for the boron free steel also gives a negative value for x. By similar reasoning, the formation of upper bainite in terms of nucleation and growth breaks down. However, the curve for the boron containing steel at 600°C yields a positive value of x and can be analyzed in terms of nucleation and growth. It is evident that boron causes a

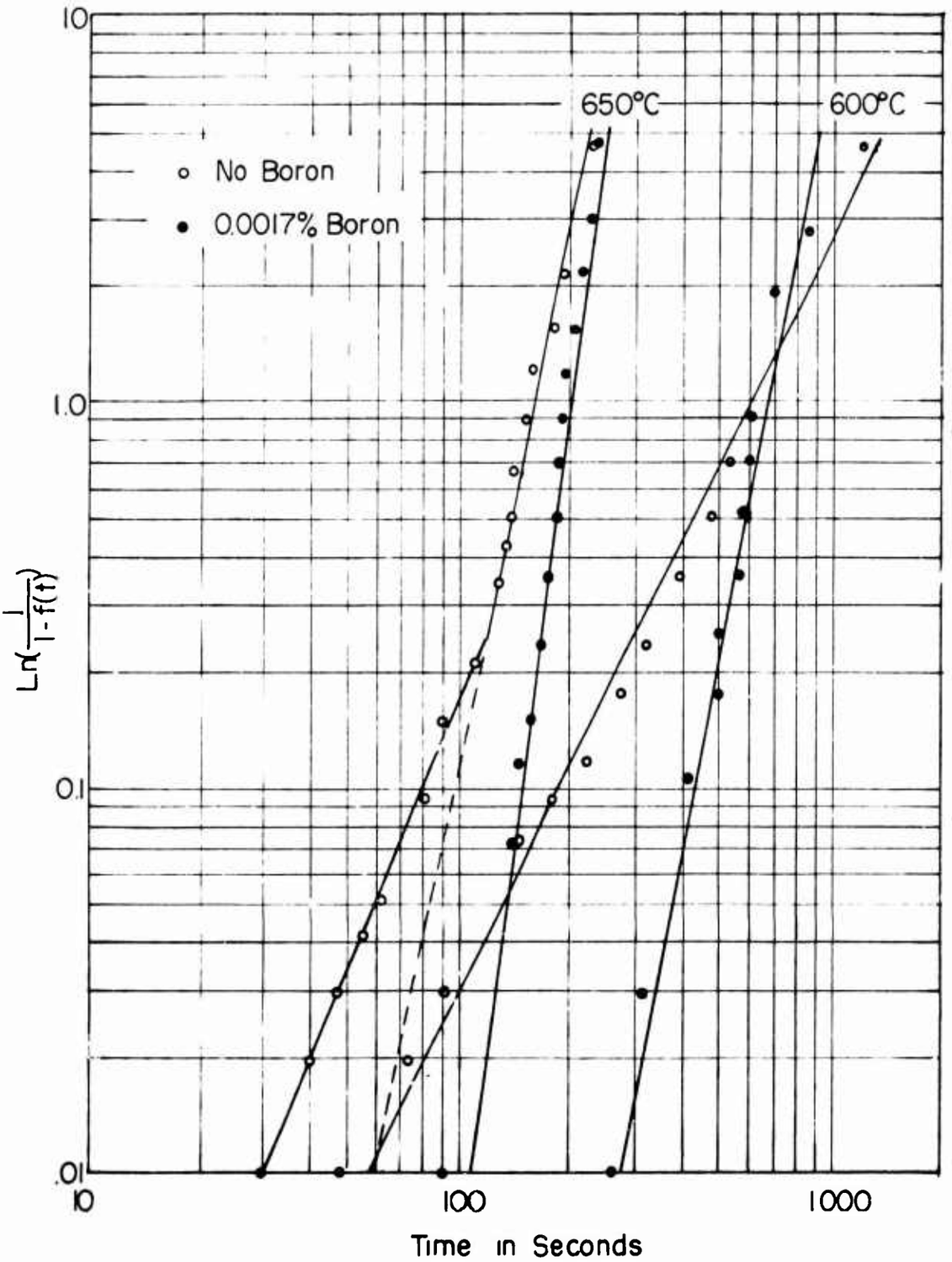

Figure 20. Plots Used for Obtaining the Equations Relating the Rate of Nucleation as a Function of Time for the Reaction Data in Figure 19.

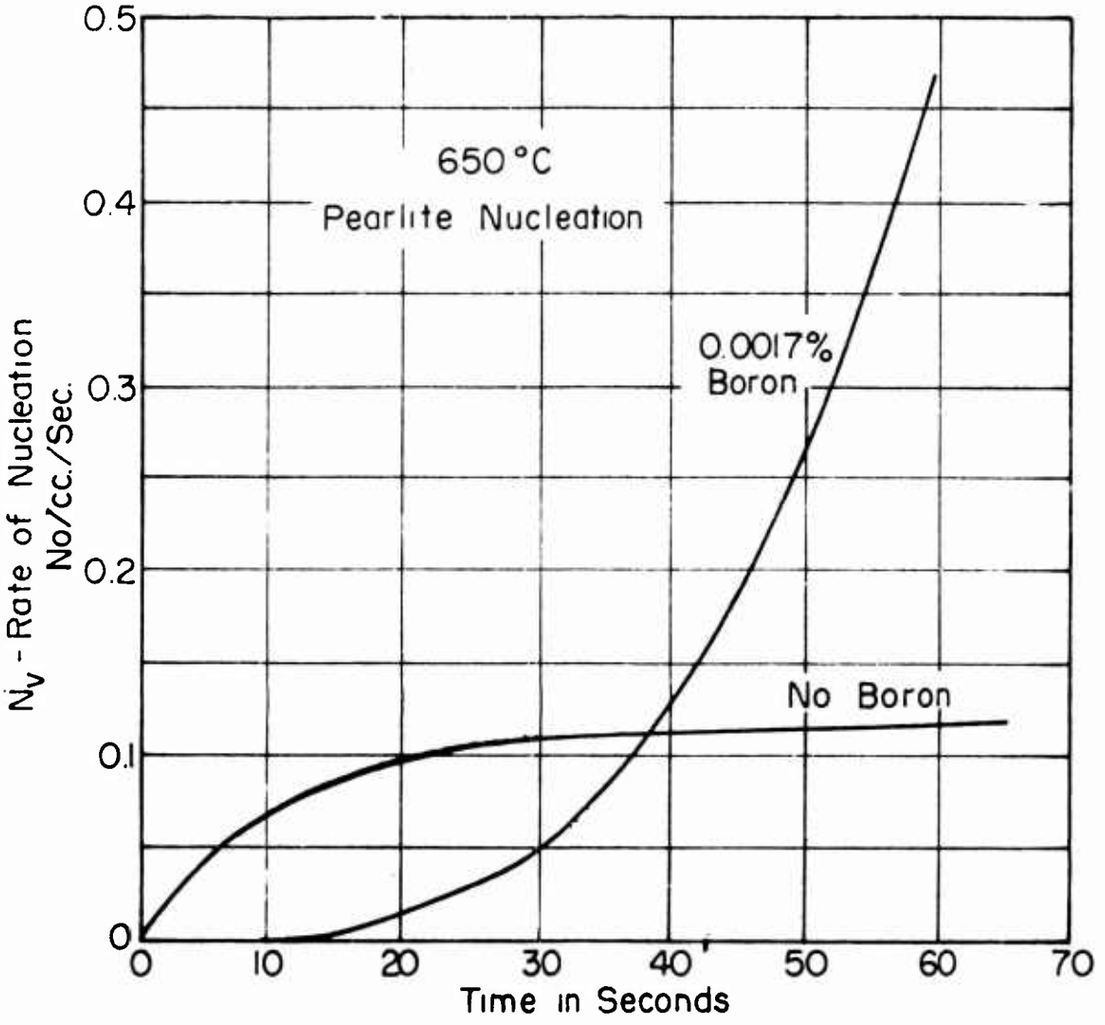

Figure 21. Plot of Rate of Nucleation as a Function of Time for the Pearlite Reaction at 650°C for the Mn-Cr-Si Steel

considerable delay in the start of the transformation. It must be concluded that boron has a potent effect in suppressing the formation of upper bainite. Furthermore, the effect at this temperature is such that the mode of transformation is apparently changed completely from upper bainite formation to pearlite formation. Since no microstructures were available, this tentative conclusion is based entirely on kinetics. Interestingly, it is only in this region that boron has an appreciable effect on the time for completion of transformation. Simply as a prediction, it is proposed that this effect on time for completion of transformation arises from the suppression of the upper bainite formation in favor of transformation to pearlite.

To summarize, boron is potent in its suppression of both pro-eutectoid ferrite and upper bainite. It does not slow down the formation of pearlite. The concept of the breakdown of the analysis of the transformation to pro-eutectoid ferrite and to upper bainite in terms of nucleation and growth is of fundamental importance. There are at least two arguments applicable to this behavior. The first states that the analysis breaks down simply because of a change in morphology. Since 650°C corresponds to the nose of the diagram, the pro-eutectoid ferrite may be the Widmanstätten type and fails to fit N and G analysis because of its acicular form. Upper bainite is definitely acicular in form. The second argument deals with two different fundamental processes, namely (a) nucleation and growth, and (b) nucleation and shear. In this concept, the N and G analysis of pro-eutectoid ferrite and bainite formation fails because these products form by the fundamentally different process of nucleation and shear. In this process, the kinetics of transformation depends on the rate of nucleation. The second argument is preferred as will be discussed in a later section.

K. HARDENABILITY MECHANISMS OF ALLOYING ELEMENTS

From the previous discussions, boron acts fundamentally in suppressing the transformation of austenite to pro-eutectoid ferrite and upper bainite. It is in order now to discuss the current state of knowledge concerning the actual mechanisms by which alloying elements contribute to the hardenability of heat treated steels.

A study of the literature leads to the conclusion that these basic mechanisms have been only partially clarified. It is generally agreed that pearlite is nucleated by cementite and bainite by ferrite. The formation of pro-eutectoid ferrite, pearlite and bainite are treated as nucleation and growth processes,[93] whereas the martensite formation is treated as a nucleation and shear process.[94] Most of the previous quantitative work on transformations has consisted of the measurements of the rates of nucleation and growth of pearlite as a function of temperature. Such work can evaluate the effect of an alloying element on the rate of nucleation and rate of growth, but contributes only in an indirect manner to the knowledge of the basic mechanisms.

A significant advance of the knowledge of these basic mechanisms was made by the Climax Molybdenum Research Laboratory on the alloying

element molybdenum.[95,96,97,98,99] Molybdenum is of particular interest in that it has considerable effect of retarding both ferrite and pearlite and it affects the upper part of the transformation diagram very much more than the lower part.

The pearlite reaction is considered first. Since the rate of growth of pearlite is mainly a function of the rate of diffusion of carbon in austenite, it is logical first to ask if molybdenum acts to slow down the diffusion of carbon, particularly since it is a strong carbide former. It was found that at high temperatures, molybdenum accelerated diffusion of carbon, at intermediate temperatures it had no measurable effect, and at lower temperatures it decreased it somewhat. In the 0.80% Mo, 0.85% C steel studied, the maximum effect of molybdenum occurs at 566°C. At this temperature the time of completion of transformation is increased 28,000 fold as compared to the plain carbon steel. However, the diffusivity of carbon is diminished only about 5 fold by the molybdenum. Thus the effect of molybdenum on the diffusivity of carbon is essentially a negligible factor. It was found, however, that molybdenum partitions to the carbide phase in pearlite in increasing amounts as the molybdenum content is increased. Up to about 0.50% Mo the carbide retains the cementite structure; above this amount the cubic $(Fe,Mo)_{23}C_6$ carbide phase forms in the pearlite. Since the diffusivity of molybdenum in austenite is low (10^{-11} cm^2 per sec), the pearlite hardenability effect then is due to the slow diffusion of molybdenum in austenite to the advancing carbide plates. Hultgren[100] has reported a similar partitioning of manganese to the carbide phase in pearlite. Thus as a principle, an alloying element would be expected to retard pearlite formation if it is a carbide former which partitions to the carbide and which has a low order of diffusivity in austenite.

The possibility of partitioning of molybdenum in ferrite was also investigated. It was found that the time for start of the transformation to pro-eutectoid ferrite increases as the molybdenum content increases. Thus, for a hypoeutectoid steel containing 0.94% Mo, the time for start of transformation at 705°C is about 5 times the start time of the same base alloy with 0.24% Mo; the start time for ferrite is delayed in direct proportion to the molybdenum content. It was further found that the molybdenum content of the ferrite was exactly that of the austenite and no partitioning effects occurred in the formation of ferrite. Thus the molybdenum effect on ferrite formation is a solid solution effect. In connection with the lack of partitioning of molybdenum, it is interesting to note that molybdenum is more soluble in alpha iron than in gamma iron and arguing

from the solubility viewpoint there is no need for molybdenum to partition in forming proeutectoid ferrite. The maximum solubility of carbon in ferrite is 0.01%. On this basis it would be argued that carbon must partition essentially completely to the austenite in forming ferrite. This is in fact the observed behavior. The degree of partitioning is less in upper bainite and nil in lower bainite and martensite. From this argument a tentative principle for partitioning in ferrite formation can be stated: it is expected that an element in solid solution in austenite should partition to the austenite during ferrite formation to the extent of its solubility in alpha iron.

Bowman[99] offers the following possibilities of explaining the effect of molybdenum on ferrite formation:

(1) Direct effect of molybdenum on the diffusion of carbon is small.

(2) May affect the carbon gradient at the ferrite-austenite interface.

(3) May reduce the solubility of carbon in ferrite, thus causing more carbon to diffuse to form ferrite.

(4) Molybdenum may slow down the basic gamma-alpha transformation in iron.

Based on arguments presented in the next section, the writers prefer the last possibility as the explanation, namely the effect of molybdenum in solid solution on the basic gamma-alpha transformation in iron.

L. THE MECHANISM OF THE TRANSFORMATION OF AUSTENITE TO FERRITE

From the preceding sections, it is evident that the effect of boron in increasing the hardenability of steels arises from its effect in suppressing the formation of pro-eutectoid ferrite. It is important next to consider the mechanism of formation of ferrite.

As previously stated, the formation of pro-eutectoid ferrite is generally considered to proceed by nucleation and growth. Thermodynamically stable nuclei of ferrite are formed which then grow by diffusion of iron atoms across the austenite-ferrite interface. Since ferrite forms isothermally, then it follows that ferrite must be nucleated by thermal nucleation (nuclei which come into being with time at the reaction temperature). The sequence of events in the formation of ferrite is not clear. Obviously two steps are required: (a) the carbon content must be reduced to very low values in the vicinity of the nucleus, and (b) face centered iron must transform to body centered iron. It can be argued that (a) precedes (b), or conversely that (b) precedes (a). In the latter case, the transformation must occur with the carbon in solid solution, which then diffuses to the austenite through the body centered lattice. However,

in this case it is most likely that the excess carbon would precipitate as the carbide in the ferrite instead of diffusing to the austenite. This is not the observed behavior; ferrite is essentially free of carbide particles. Thus, one is forced to conclude that the carbon diffuses away before the transformation occurs. However, the upper bainite reaction occurs with only a part of the carbon diffused away and martensite forms with all of the carbon in solid solution.

This leaves the more important question as to the basic mechanism of the transformation from face centered to body centered iron. If we accept the mechanism of nucleation and growth, then ferrite nuclei form and grow by diffusion of iron atoms across the interface. The diffusion of iron is relatively slow, an order of magnitude of 10^{-13} cm^2/sec at the Ae_3 temperature and decreases rapidly with temperature. To explain the observed maximum in the rate of ferrite formation, one must argue entirely on a maximum in the rate of nucleation.

Hultgren[100] proposes a somewhat different explanation for the formation of ferrite. In pure iron he proposes the existence of embryo of alpha iron which form by statistical fluctuations both above and below the equilibrium temperature. In the gamma iron region, there is no stable size for alpha iron nuclei. Below the transformation temperature, the embryo can grow to stable size and become nuclei which continue to grow by diffusion. When gamma iron contains carbon in solid solution, he resolves the difficulty of the concentration requirement for ferrite also through statistical fluctuations in the carbon content. It would seem, however, that the probability of simultaneous occurrence of the two events in a given embryo would be extremely low.

There are serious objections to the concept of ferrite formation from austenite as a process of nucleation and growth. The major objections will be discussed under three general topics: (a) orientation relationships, (b) kinetics of the reaction, (c) reversibility of the reaction.

1. Orientation Relationships

Mehl and Smith[101] found a lattice orientation relationship in ferrite formed from gamma iron in pure iron. This is the Kurdjumow and Sachs relationship, namely

$$\{111\}_\gamma \parallel \{110\}_\alpha$$
$$[110]_\gamma \parallel [111]_\alpha$$

It is of interest to note that gamma iron cannot be retained even by the most drastic quenching. This fact is difficult to rationalise on the basis of nucleation and growth since after passing through the temperature range of the maximum rate of nucleation, the rate of nucleation continuously decreases as does the rate of growth. The same lattice orientation relationship was found for pro-eutectoid ferrite.[102] Bainite was found to obey either the Kurdjumow and Sachs relationship or the Nishiyama relationship[103] which is

$$\{111\}_\gamma \parallel \{110\}_\alpha$$
$$[211]_\gamma \parallel [110]_\alpha$$

Martensite is found to obey either of the two relationships depending upon the type of alloy studied. Thus the body centered decomposition products pro-eutectoid ferrite, bainite, and martensite all exhibit a definite orientation relationship with the austenite from which they form. Martensite is considered here as a ferrite structure which is distorted by the carbon in solid solution.

The presence of these orientation relationships is difficult to reconcile using the nucleation and growth mechanism. The nucleation theory imposes no orientation requirements on the embryo which eventually grow into stable nuclei. These embryo are conceived as either springing into being (as in gases), or attain a certain size by atom to atom additions. No sound argument appears in the literature to explain the lattice relationships observed for ferrite or the other products in terms of nucleation and growth.

2. Kinetics of Ferrite Formation

Surprisingly little quantitative data on the kinetics of formation of pro-eutectoid ferrite can be found in the literature. Most of the quantitative work on the decomposition of austenite has been done on the formation of pearlite. It may be presumed that in part the argument for ferrite forming as a nucleation and growth process arises from the nature of the martensitic transformation. Martensite formation in heat treatable steels is essentially time independent and proceeds by a shear mechanism. Therefore any other decomposition that proceeds isothermally with time can be looked upon as proceeding by nucleation and growth. It will be later demonstrated that kinetics is not a reliable criterion for a martensitic or shear transformation.

Quantitative measurements on the rate of ferrite formation in hypoeutectoid steels were made by McBride, Herty, and Mehl.[104] The study was concerned with the effect of silicon deoxidation and aluminum deoxidation on the rate of ferrite formation. Twelve plain carbon steels were studied covering a range of carbon of 0.33 - 0.50 per cent. The data were with some exceptions analyzed satisfactorily in terms of a first order reaction which states that the rate of reaction is proportional to the amount of reactant (austenite) remaining. The equation used is

$$dF/dt = K(1 - F) \qquad (8)$$

or

$$\ln 1/(1-F) = Kt \qquad (9)$$

where

F = amount of ferrite

t = elapsed time

(1-F) = fraction of austenite remaining.

Thus, the basic relationship is apparently quite different from that for nucleation and growth. The form of the curves obtained are illustrated in the top diagram of Figure 22. The curves are not the sigmoid type characteristic of nucleation and growth processes. The flat initial part of the curve arises from the uncertainty of zero time at the reaction temperature.

The difference in grain size was taken into account by dividing the rate constant K by the grain surface per unit volume S. The logarithm of K/S is plotted against the reciprocal of the absolute temperature in Figure 23 for a silicon killed steel and on aluminum killed steel. It will be noted that the rate of ferrite formation increases with decreasing reaction temperature. Also, even with the grain size taken into account, the ferrite forms more slowly in the silicon treated steel. No explanation of this effect was attempted in the paper. It is suggested here that nitrogen in solid solution is effective in restraining the formation of ferrite from austenite. In the silicon steel, it would be expected that nitrogen would be essentially in solid solution in austenite. Aluminum, on the other hand, is a strong nitride former and in aluminum deoxidized steels the nitrogen would be mainly tied up as aluminum nitride.

In Figure 23, along with the K/S values are plotted the rates of diffusion of carbon in alpha and gamma iron, and the rate of self-diffusion of gamma iron. It will be noted that as the reaction temperature is decreased the rate of formation of ferrite increases, but the rate of diffusion of carbon in gamma iron decreases. Thus, in the formation of ferrite from austenite, the diffusion of carbon in austenite is not the rate controlling factor. It still may be argued from nucleation and growth that the increasing rate of ferrite formation results from an increasing rate of nucleation. However, the rate of growth which would depend on diffusion of iron would be very slow. It should be pointed out that K/S cannot be directly compared with self-diffusion rates of gamma iron.

Kulin and Speich[105] have made a significant contribution to the understanding of the martensitic or shear transformation. They studied the martensite formation in an essentially carbon free iron--14% chromium--9% nickel alloy at reduced temperatures. It was found that martensite readily forms isothermally, in contrast with the previous concept of a temperature dependent reaction. Isothermal martensite formation has been reported by other investigators. Typical curves for the isothermal formation of martensite are presented in the bottom diagram of Figure 22. The similarity of curves for isothermal martensite formation and isothermal ferrite formation is striking. Both are distinctly different from sigmoid curves typical of nucleation and growth processes.

The logarithm of $\ln\left(\frac{1}{1-f_{(t)}}\right)$ is plotted against the logarithm of time for the various ferritic reaction products in Figure 24. This is the type of plot previously used to analyze the rate of nucleation in a nucleation and growth reaction. The data for ferrite at the knee and upper bainite are those of Gudtsor and Nazarov;[89] the data for pro-eutectoid ferrite between Ae_3 and Ae_1 are after McBride, Herty, and Mehl,[104] and martensite from

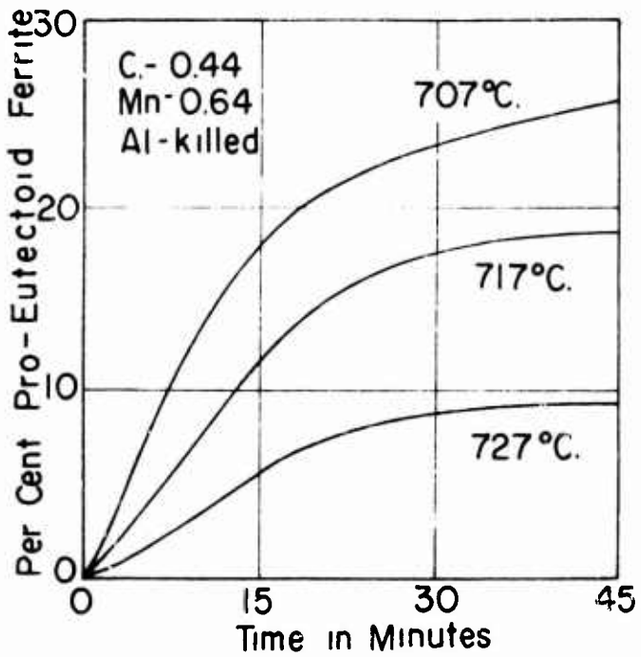

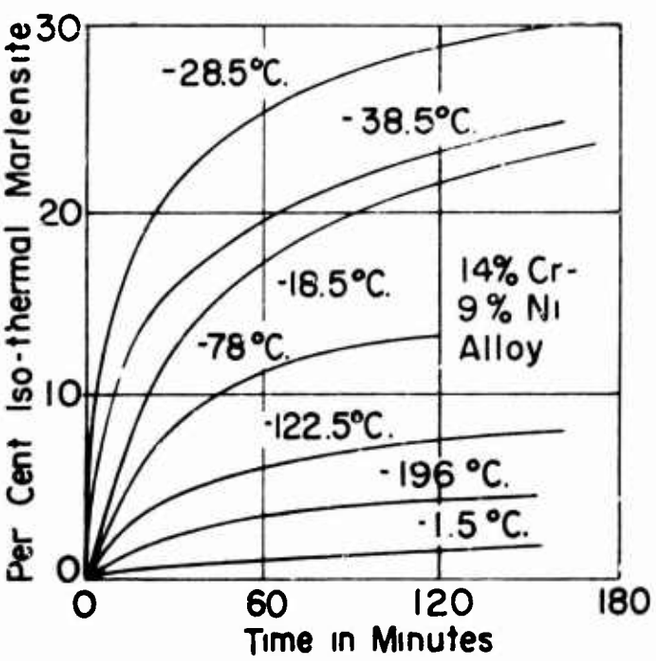

Figure 22. Kinetics of Isothermal Formation of Pro-Eutectoid Ferrite (upper diagram) and of Isothermal Formation of Martensite (lower figure)

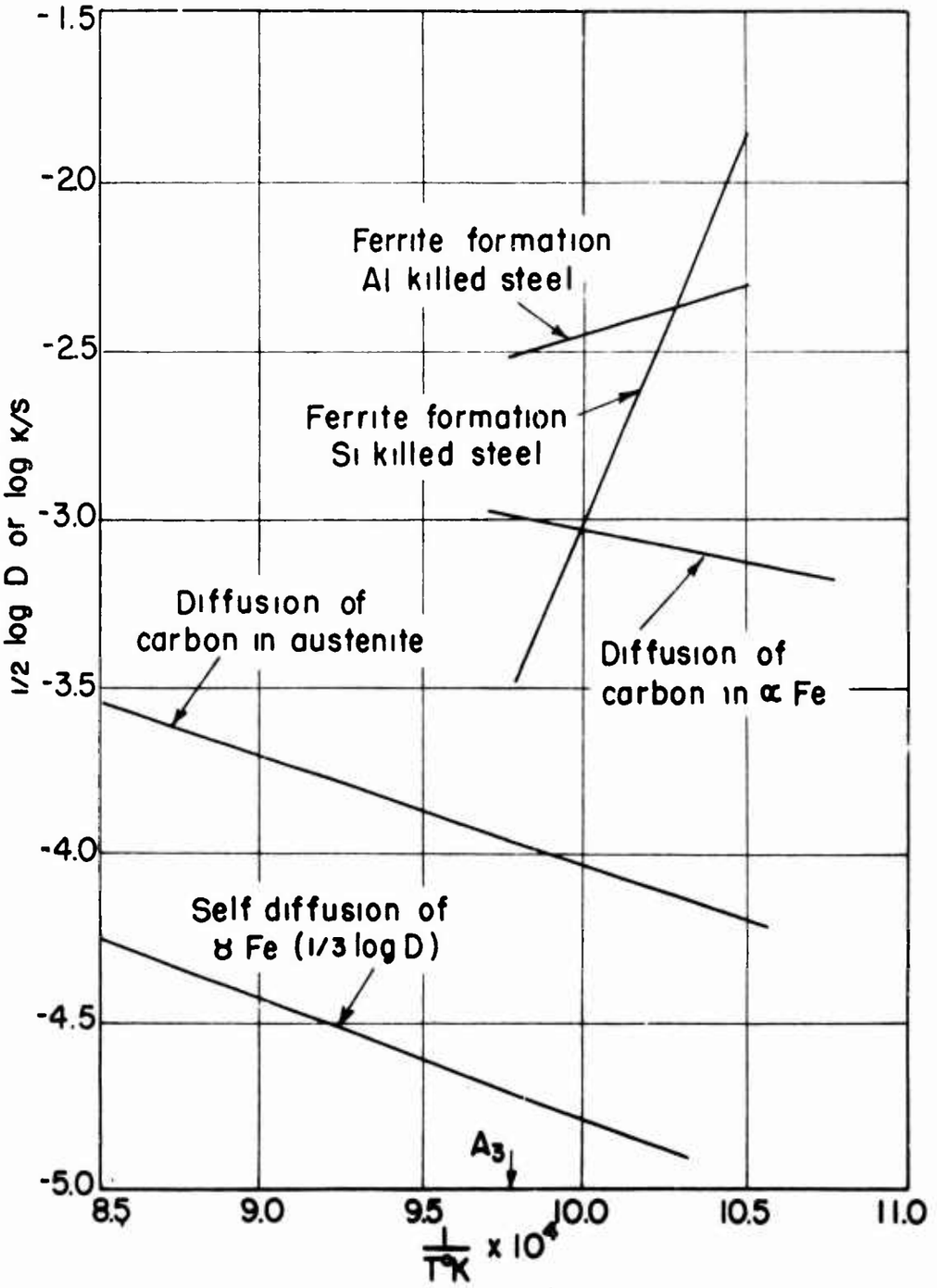

Figure 23. Kinetics of Pro-Eutectoid Ferrite Formation in a Carbon Steel Deoxidized with Silicon, Aluminum

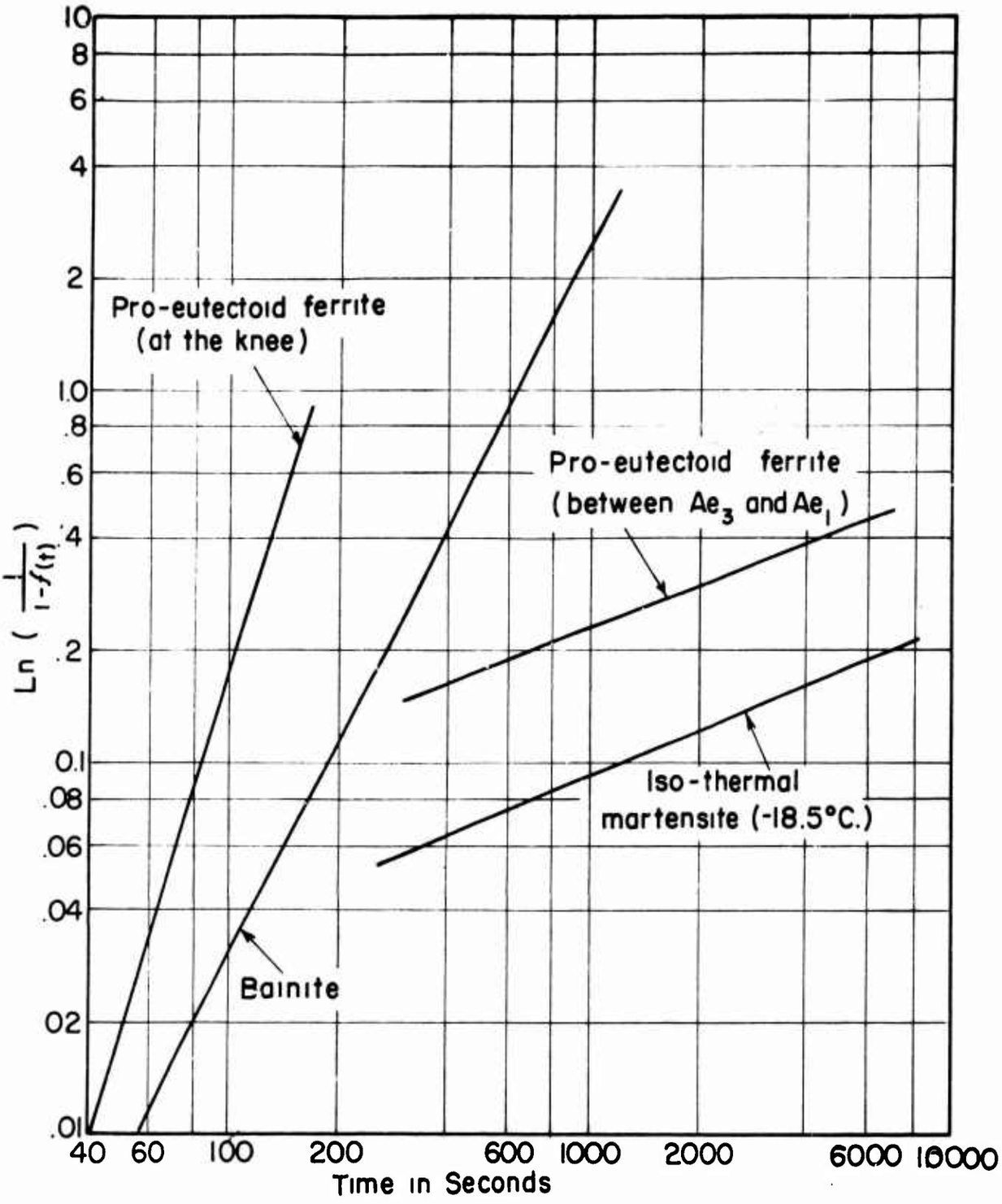

Figure 24. Analysis of Kinetics of Isothermal Formation of Pro-Eutectoid Ferrite, Upper Bainite, and Martensite

Kulin and Speich.[105] It will be recalled that analysis in terms of nucleation and growth broke down for ferrite at the knee and for upper bainite. Such is also the case for pro-eutectoid ferrite between Ae_3 and Ae_1 and for martensite. It is postulated here that all these reactions proceed by nucleation and shear. From these plots, it is evident that the rate of shear nucleation goes through a maximum with decreasing reaction temperature.

The observation of isothermal martensite formation is of fundamental importance. The previous concept of time independence as a necessary criterion for the martensitic reaction is not valid, since shear transformation can proceed with time at a constant temperature. It is believed that isothermal martensite formation proceeds with difficulty in heat treatable steels because of the comparatively large amount of carbon in solid solution in austenite which suppresses the shear into martensite. Steels containing up to 0.6 per cent carbon have been made to transform isothermally to martensite at sufficiently low temperatures. Thus, a martensitic transformation must be established on the basis of the mechanism (absence of diffusion in the common sense) and on the reversibility of the transformation.

3. Reversibility of the Ferrite Transformation

Nehrenberg[106] has made a valuable contribution to the establishment of the reversibility of the ferrite reaction in steels. He found that the shape of the austenite formed just over the Ae_3 temperature is entirely dependent upon the shape of the ferrite from which it is formed. A martensitic steel has an acicular ferrite matrix and accordingly the austenite formed is acicular. Likewise, a steel transformed in the pearlite range has an equi-axed ferrite matrix which subsequently forms equi-axed austenite. It was observed that the transformation does not cross over into an adjoining grain. Thus, it is a transformation in situ. Such behavior seemingly can be explained only in terms of a fundamental shear mechanism of transformation. This work also demonstrates the reversibility of the martensite reaction, despite the fact that the excess carbon is precipitated as a carbide on reheating to the austenite range.

From the above arguments, one is forced to conclude that ferrite is formed by a shear mechanism, as are bainite and martensite. Pearlite is the only decomposition product that forms by nucleation and growth. An impediment to the acceptance of ferrite formation as a shear transformation is the variety of morphological shapes that it forms. However, it is expected as will be discussed that because of increased atomic thermal vibrations with increasing temperature, the length of the individual shear will become shorter. At the lower limit, martensite shears completely across the grain. These short shear paths can lead to a variety of shapes. Kurdjumow[107] has presented a strong argument for various morphologies being formed by shear transformations. It is significant in this connection that ferrite usually does not form a spherical shape as might be expected for the growth of a nucleus. Also, in the interpretation of the kinetics of ferrite formation in terms of a first order reaction, the fraction of austenite remaining is also roughly proportional to the amount of austenite-ferrite interface for a spherical grain. One would expect a shear to initiate more easily at an interface because of the presence of excess strain energy.

It would appear that most of the fundamental transformations in metals should proceed by shear. A tentative principle might be stated that a transformation is expected to proceed by shear except if (a) the new lattice is considerably different in symmetry, and (b) the new phase has a significantly different composition.

M. THE BORON HARDENABILITY EFFECT

In formulating a working hypothesis for the mechanism for the boron hardenability effect, two factors stand out as being basically important. These are that boron acts principally in suppressing the formation of ferrite and upper bainite and that the fundamental mechanism is a shear mechanism. It follows then that the boron effect is a solid solution effect arising from exceptionally high strain energy peaks in the vicinity of the boron atoms. In general, introducing an interstitial solute atom into the iron lattice introduces strain energy the magnitude of which is proportional to the difference in the size of the solute atom and the size of the interstitial hole. It is postulated that these localized energy peaks increase the resistance to the fundamental shear mechanism.

In this connection, it is interesting to estimate the expected relative effects on ferrite formation of the interstitial solute atoms carbon, nitrogen, and boron. These calculations are based entirely on the solubility of these elements in gamma and alpha iron. The magnitude of the strain energy effect is taken as being inversely proportional to the solubility. This of course assumes that the solubility limit depends entirely on the strain energy effect. The maximum solid solubilities in atomic per cent of carbon, nitrogen, and boron in alpha and gamma iron are listed in Table IV. The strain energy factor in column C is based on the solubilities in gamma iron. Since nitrogen is most soluble, it is given a factor of one. The factors for carbon and boron are calculated by dividing their respective solubilities into that of nitrogen. The next problem is the amount of these elements present when gamma iron transforms to alpha iron, that is, the degree of partitioning in the formation of ferrite. The best assumption appeared to be that these elements partition to the extent of their maximum solubilities in alpha iron. Therefore, the effectiveness factor was calculated by multiplying column A by column C. The results indicate that carbon is least effective in suppressing ferrite formation. Nitrogen is four times as effective and boron is forty-three times more effective than carbon!

Corroboration of the greater effectiveness of nitrogen as compared to carbon is found in the work of Bose and Hawkes[108] on the kinetics of the eutectoid decomposition in the iron-nitrogen system. At the nose of the curve, the eutectoid composition (2.35% N) started to form a pearlite structure after 15 seconds. This is compared to about one second for eutectoid steel. Interestingly, the hypo-eutectoid compositions did not form ferrite but transformed directly to pearlite. This behavior substantiates the concept of nitrogen as an effective agent in suppressing the formation of ferrite It was previously pointed out that nitrogen in solid solution is the probable explanation of the difference in rate of ferrite formation in silicon deoxidized steels and aluminum deoxidized steels.

TABLE IV

Calculations of Effectiveness Factors for Carbon, Nitrogen, and Boron on the Transformation of Gamma to Alpha Iron

Element	A Maximum Solubility in Fe-a/o	B Maximum Solubility in Fe-a/o	C Strain Energy Factor	Effectiveness Factor A X C	Ratio to Carbon
Carbon	0.088	8.673	1.207	0.107	1
Nitrogen	0.397	10.469	1.000	0.397	4
Boron	0.016	0.036	289.903	4.636	43

The role of the extent of partitioning in determining the degree of effectiveness of an element in suppressing ferrite formation is important. If the solubility of an element is greater in gamma iron than in alpha iron, then partitioning of the atom will occur in forming ferrite to the extent of its solubility in alpha iron and a maximum effect will be observed beyond which concentration no further effect will be realized. Thus, an optimum concentration of boron is observed for maximum hardenability which depends upon the solubility of boron in alpha iron at a reaction temperature corresponding to the nose of the curve. This principle follows also for carbon. In comparing SAE 1019 steel (0.17 C, 0.92 Mn) with SAE 1050 steel (0.50 C, 0.91 Mn),[69] the time for start of formation of pro-eutectoid ferrite 200°F below the Ae_3 temperatures is two seconds for both steels. Thus, the effectiveness of carbon is restricted by its low solubility in alpha iron and the high degree of partitioning in ferrite formation. In the opposite case in which the solute is more soluble in alpha iron than in gamma iron, no partitioning in ferrite formation is expected and the effect on ferrite formation should be proportional to the concentration. Molybdenum is a good example of this type of solute atom. The maximum solubility of molybdenum in gamma iron is 3% by weight and 1.77 atomic per cent. Referring to Table IV this gives molybdenum a strain energy factor of 5.9 which places it between nitrogen and boron in the degree of straining of gamma iron. Since the solubility of molybdenum in alpha iron is large, the ferrite effect should be proportional to the concentration. A 0.8 Mo - 0.4 C steel (0.36 C, 0.17 Mn, 0.82 Mo) is compared with a 0.2 Mo - 0.40 C steel (0.42 C, 0.20 Mn, 0.21 Mo).[69] The time for start of ferrite formation 100°F below Ae_3 for the 0.2 Mo. steel is 5 seconds, and for the 0.8 Mo steel is 20 seconds. Thus, the effect of molybdenum on suppression of ferrite formation is proportional to the concentration. This strong effect of molybdenum on ferrite formation may be the fundamental reason why it partitions to the carbide phase in pearlite formation. Its potent effect on both ferrite and pearlite formation makes it an outstanding alloying element for the upper part of the transformation temperature range.

The kinetics of the formation of upper bainite warrants some discussion. It will be recalled from Figure 19 that a highly distorted sigmoid curve is obtained to describe the isothermal reaction in this range. This is a different form of curve from that for ferrite and martensite. It will be recalled that the rate of formation of pro-eutectoid ferrite apparently is not controlled by the rate of diffusion of carbon in austenite. However, this diffusivity is decreasing rapidly as the reaction temperature is lowered and one would expect that at some temperature range the diffusion of carbon will influence the reaction kinetics. This apparently happens in the upper bainite curve and the reaction curve can be interpreted as the summation of two factors, (a) rate of diffusion of carbon in austenite, and (b) rate of nucleation of shear.

From the previous arguments, the diminishing effectiveness of boron with increasing carbon content can be rationalized. The argument mainly stems from the fact that boron acts only in suppressing ferrite formation and as the carbon content approaches eutectoid composition, the amount of ferrite that forms decreases. The concept of boron acting to retard ferrite formation is substantiated by the general observation that boron steels characteristically show less ferrite in the structure. The probability of

nucleating pearlite increases as the carbon content increases. At low carbon contents, considerably more ferrite must be formed before cementite is nucleated. As the carbon content approaches eutectoid, very little enrichment of austenite by ferrite formation is required before cementite is nucleated. According to these arguments, the boron effect should become zero at the eutectoid composition. Also, boron should be expected to have no effect on the start time of decomposition to pearlite in the hypereutectoid steels. Finally, boron should not be expected to affect the rate of pearlite formation because even if it partitions to the cementite, its diffusivity is comparable to that of carbon. A possible secondary effect may be a reduction of solubility of boron in gamma iron with increasing carbon content.

The proposed boron mechanism has interesting engineering ramifications. The effect is principally a delay in the start of transformation. Boron then should be an effective alloy substitute in engineering parts of such geometry that all points in it cool at rates in excess of the critical cooling rate. However, in slack quenched parts, the hardness will fall off more rapidly in the interior of the part and in this case boron is expected to be inferior to the substitutional solute atoms such as manganese, chromium, and molybdenum which also affect the pearlite reaction. Also, boron would be expected to be ineffective in carburized cases with carbon contents in excess of the eutectoid composition.

M. STRAIN ENERGY EFFECTS IN INTERSTITIAL SOLID SOLUTIONS

Since the effect of boron in suppressing the shear transformation of gamma to alpha iron depends upon the exceptionally high strain energy peaks associated with the boron atoms in solid solution, some calculations will be made on strain energy effects of carbon, nitrogen, and boron dissolved interstitially in gamma iron.

The first problem that arises is that of obtaining the effective diameters of these atoms in gamma iron. These effective diameters depend upon the environment in which they are placed. The best approach seemed to be to calculate the effective diameters from the measured expansion of the gamma lattice. The interstitial spaces in the face centered lattice are at the middle of the edges and at the center of the lattice. These positions are all equivalent and are of the size $0.293\ a_o$, where a_o is the lattice parameter. The increase in a_o of gamma iron with carbon is given as

$$\Delta a_o = 0.0027 \times (\%C \times 10) \text{ in } K_x \text{ units} \qquad (10)$$

For 0.01% carbon, the ratio of iron to carbon atoms is 2149:1. The number of unit cells per carbon atom is 537. The size of the interstitial hole in gamma iron is 1.0665 Kx units. Of the three possible edges, on the average, one out of three carbon atoms go into one particular edge, expanding the lattice in this direction. Each carbon atom is shared by four unit cells. If V is the effective diameter of carbon, then

$$\frac{V - 1.0665}{3} \times \frac{4}{537} = 0.00027 \qquad (11)$$

$$V = 1.178\ K_x \text{ units}$$

The effective diameter calculated for nitrogen in this manner is 1.1955 Kx units. The listed diameter for carbon and nitrogen are the following:

State	Carbon	State	Nitrogen
Covalent	1.54	Covalent	1.40
Ionized (+4)	0.58	Ionized (+5)	0.50

Thus from these crude calculations, one would calculate that carbon is about 37% ionized and nitrogen about 22% ionized.

There is a more exact method of calculating the effective diameters. The relation between the lattice parameter, the per cent interstitial solute atom, and the diameter of the solute atom can be formulated from the elastic theory of isotropic solids. In this treatment, the expansion of the interstitial hole by the larger solute atom is directly related to the experimentally determined ratio of the change in lattice parameter to the change of concentration of the interstitial atom. This relationship has been previously derived by Speiser, Spretnak, and Taylor.[109]

The relationship derived by this treatment for diameters of interstitial atoms is for the case of face centered cubic lattices the following:

$$\Delta R = \frac{\Delta V}{4\pi r^2} = \frac{3a_o^2 \Delta a}{4\pi\left(\frac{a^2}{4}\right) \cdot Z f_2} \qquad (12)$$

where

ΔR is the increase in the radius of the interstitial hole as a result of inserting the solute atom

a_o is the observed expansion of the interstitial alloy

a is the lattice parameter of the alloy

Z is the number of solvent atoms per unit cell

f_2 is the ratio of solute to solvent atoms in the crystal.

The effective diameter of the interstitial atom in solid solution in face centered lattices is

$$d = \left(a_o - \frac{\sqrt{2}}{2} a_o\right) + 2\Delta R = 0.293 a_o + 2\Delta R \qquad (13)$$

For carbon in gamma iron, the effective diameter is 1.32 Å and for nitrogen

1.42 Å. Thus by these more exact calculations carbon in gamma iron is about 23% ionized and nitrogen is either neutral or slightly negatively ionized. It is to be noted that carbon requires a smaller hole than does nitrogen. This is in agreement with the observations of Jack[110] who found that nitrogen in interstitial solid solution has a radius of 0.7 Å. He also observed that the lattice parameter of the compound Fe_2C increased as carbon was replaced by nitrogen.[111]

No parameter data were available for boron in gamma iron to calculate its effective diameter. However, it can be inferred that the boron atomic diameter in gamma iron is in the range 1.80 - 1.90 Å. This follows from a study of the behavior of boron in its compounds. It is well known that boron has more stable orbitals than valence electrons, i.e. it tends to increase the electron density in its vicinity. Boron then would tend to be neutral or slightly negative in combination with elements such as iron. This is further substantiated from the fact that although many interstitial compounds such as CrN, FeO, TaC, TiC, TiN, TiO, UN, VC, have a sodium chloride structure (which implies a covalent bond), FeB on the other hand is a distorted NiAs structure (orthorhombic) which is characteristic of interstitial compounds formed with a transition element and a rather electronegative element. Furthermore, boron has a very strong tendency to form chains (FeB) and sheets (TiB_2, ZrB_2, CbB_2, TaB_2, and VB_2), and cage-like structures in compounds such as CeB_6 and LaB_6. Consequently, it is reasonable to expect that boron is un-ionized or slightly negatively ionized in iron. Thus a diameter of 1.85 Å for boron in interstitial solid solution is reasonable. From the above arguments, the solubility of boron is dependent essentially on its size since its electronegativity is 2.0 compared to 2.1 for iron, whereas the electronegativity for carbon and nitrogen is 2.5 and 3.0 respectively. Thus the difference in solubility of carbon and nitrogen is undoubtedly due in part to their electronegativities. This is borne out by the relatively large change in solubility of carbon and nitrogen in gamma iron with temperature compared to the relatively low change for boron.

The strain energy introduced by an interstitial solute can be calculated by the well known equation of Mott and Nabarro

$$\Delta S = 8\pi r_0 (r - r_0)^2 GN \qquad (14)$$

This equation arises from the assumption that the solid solution is an elastic medium in which the interstitial positions are holes of radius r_0. Then the strain energy is the work necessary to force N spheres of radius r into N holes. G is the modulus of rigidity. The strain energy per atom then is

$$\Delta S = 8\pi r_0 (r - r_0)^2 G \qquad (15)$$

For the calculations, a value of G for gamma iron was estimated from data in the Metals Handbook (ASM) for alpha iron. The data are as follows:

	$S_{11} \times 10^{-13}$	$S_{12} \times 10^{-13}$	$S_{44} \times 10^{-13}$	
α Fe	7.57	-2.82	8.62	$cm^2/dyne$

G is calculated from the expression

$$\frac{1}{G} = S_{44} + 4(S_{11} - S_{12} - \tfrac{1}{2} S_{44}) \qquad (16)$$

The calculated value of G is 3.02×10^{11} dynes/cm^2. This value must be reduced about 40% in the gamma range, as indicated by experimental work on the modulus of elasticity for iron as a function of temperature. Hence an approximate value of G is taken as 1.8×10^{11} dynes/cm^2.

The strain energies calculated per atom in gamma iron are the following:

Element	Strain Energy per Atom in Ergs	Ratio
C	0.75×10^{-13}	1
N	1.48×10^{-13}	2
B	7.36×10^{-13}	10

Since these values are strain energy per atom, the values can be interpreted as the heights of the strain energy peaks at the location of the interstitial atoms. Thus, the strain energy peak is much higher for the boron atom than for carbon and nitrogen. It is also of interest to note that the peak for nitrogen is about twice that for carbon, in keeping with previously presented evidence that nitrogen is more effective in suppressing ferrite as compared to carbon.

It appears logical to presume that the effectiveness of an interstitial atom in suppressing a shear transformation should also depend upon the number of unit cells affected by the atom. The magnitude of the strain energy as a function of the distance from the solute atom is calculated by the following method.

The strain energy is given by the expression

$$\Delta S = 8\pi r_0 (\Delta R)^2 G \qquad (17)$$

From elastic theory, it follows that the expansion of a sphere of radius r is given by

$$\Delta R = \frac{A \Delta R_A}{r^2} \qquad (18)$$

where

A is a constant

ΔR_A is the expansion of the interstitial hole.

Then

$$d(\Delta R) = -\frac{2A \Delta R_A}{r^3} dr$$

Integrating $$\Delta R - \Delta R_A = -2A\Delta R_A \int_{r_0}^{r} r^{-3} dr$$

$$\Delta R = \Delta R_A + \Delta R_A A \left\{ \frac{1}{r^2} - \frac{1}{r_0^2} \right\} \tag{19}$$

$$At\ r = \infty \quad \Delta R = 0$$

$$0 = \Delta R_A \left[1 + A\left(-\frac{1}{r_0^2}\right) \right]$$

$$\therefore A = r_0^2 \tag{20}$$

Therefore,

$$\Delta R = \Delta R_A + \Delta R_A \left\{ \frac{r_0^2}{r^2} - 1 \right\}$$

$$= \Delta R_A \left[1 + \frac{r_0^2}{r^2} - 1 \right]$$

$$= \frac{\Delta R_A r_0^2}{r^2} \tag{21}$$

It is convenient to express the distance r in terms of unit cells.

Let $r_0 = a_0/2$

then $r = a_0/2\, x$

where x is the number of unit cells

$$\therefore \Delta R = \frac{\Delta R_A}{x^2} \tag{22}$$

Substituting in Equation

$$\Delta S = 8\pi r_0 G \left(\frac{\Delta R_A}{x^2} \right)^2$$

$$= 4\pi a_0 G \frac{\Delta R_A^2}{x^4} \tag{23}$$

Thus, it is evident that the strain energy falls off as the fourth power of the distance expressed in unit cells.

The data used for calculating the strain energy peaks are the following:

Element	ΔR_A	ΔR_A^2
C	0.25	0.0625
N	0.35	0.1225
B	0.78	0.6084

If the strain energy peak associated with the carbon atom is assigned the value of 1.0, the peak for nitrogen is 1.96 and for boron it is 9.73. The peaks associated with the solute atoms and the manner in which the strain energy falls as a function of distance from the solute atom is illustrated in Figure 25. In order to illustrate more clearly the manner in which the strain energy falls off with distance, calculations were made on the number of unit cells which have 1% or more of the peak strain energy associated with the carbon atom. For a carbon atom 133 unit cells are so affected, 198 unit cells by a nitrogen atom, and 730 unit cells by a boron atom. It would appear that the effectiveness of an interstitial atom in suppressing shear transformations is some sort of product of the strain energy peak and the volume distorted. The nature of this effectiveness factor is not known at present, but if one assumes a straight product of these two factors, the effectiveness ratio of C:N:B would be of the order 1:3:50.

O. SOURCES OF SHEAR IN TRANSFORMATIONS

An allotropic transformation in a metal is possible only when the free energy of one modification is lower than that of the other modification. The stable phase is one with the lower free energy. This condition is a thermodynamic requirement, but the transformation is possible only if sufficient energy is available to surmount any potential barrier which hinders the transformation. In pure metals, this activation energy is very low and the transformation will proceed without difficulty.

The fundamental difference between diffusion and a phase transformation is that in the former process the atoms change their positions at random and independently (as a first approximation), whereas in the latter process the movement of the atoms is coordinated over quite large distances. Another viewpoint is that in a diffusion process the system goes from a higher state to a lower state of energy by a disordering process, whereas in a crystal transformation, the system goes from a higher state to a lower state by a cooperative process. Since the energy necessary for a crystal transformation can arise only from thermal energy and since it is evident that this is a cooperative process, this means that the mechanism by which a crystal transforms from one modification to another must be through one or more of the normal modes of vibration of the crystal which lead (with only slight adjustments of the positions of the atoms) to the new crystal modification. As a general principle, one can state that a nucleation and growth process takes place when a system passes from a disordered state to a more highly ordered state (such as the transformation from liquid state to the solid state, precipitation of a compound from solid solution). On the other hand, shear transformations (allotropic transformations) involve cooperative movement from one ordered state to another ordered state.

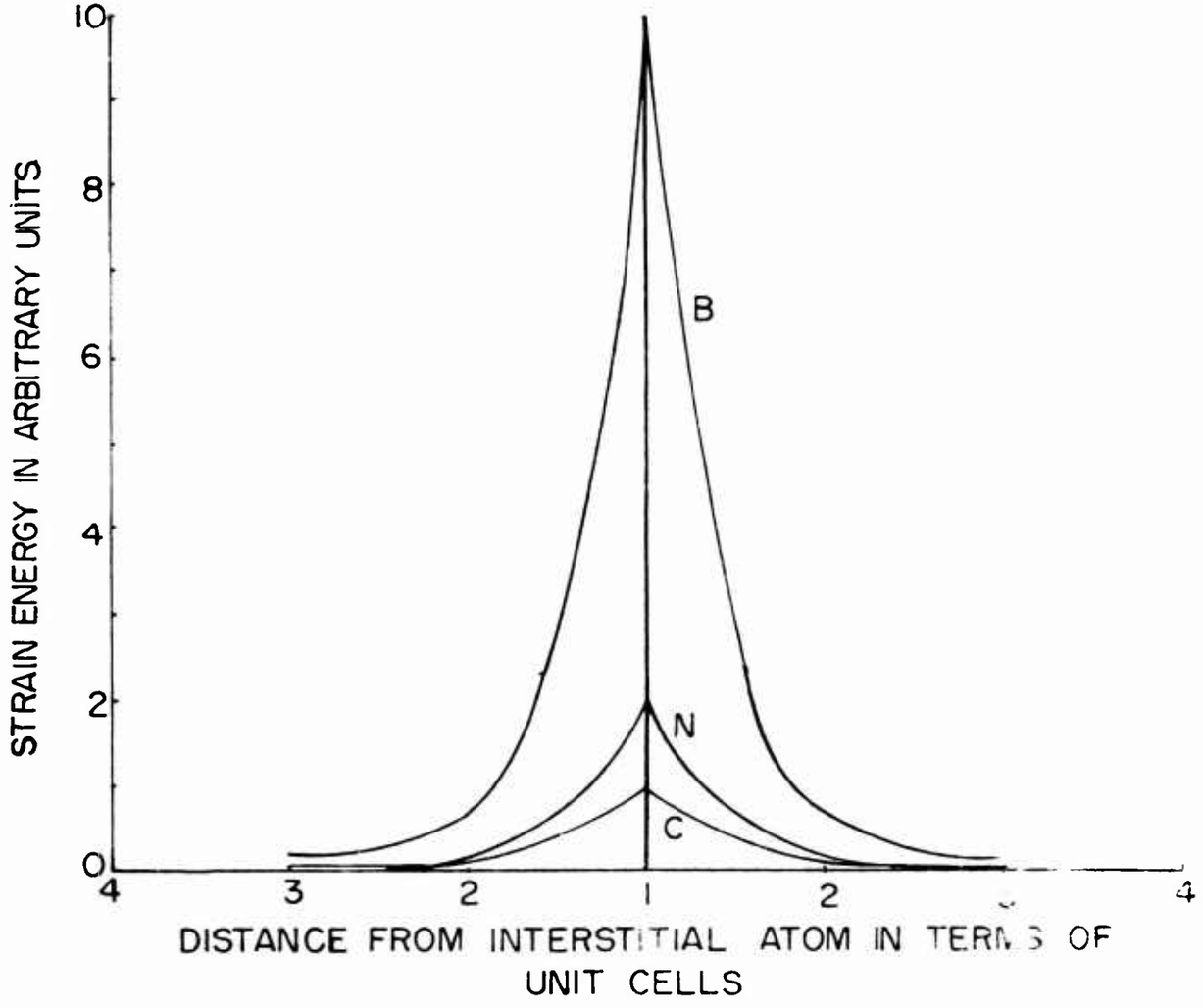

Figure 25. Strain Energy Peaks and Strain Energy as a Function of Distance from the Atom for an Atom of Carbon, Nitrogen, and Boron in Solid Solution in Gamma Iron

It can be demonstrated that these normal modes of vibration of a crystal are in their overall consequence combinations of shearing movements which lead to the formation of a new crystalline form. The length of the individual shearing path will depend upon the degree of undercooling, temperature, and the perfection of the crystal. Increasing the undercooling leads to a larger difference in free energy between the metastable and stable states. This free energy difference tends to lower the free energy barrier for transformation. However, solute atoms may cause deformations of the lattice such that the barrier is sufficiently high so that the transformation cannot proceed. It should be remembered also that lowering the temperature reduces the thermal energy, making the transformation more difficult. It would be expected that if the undercooling is large, a large number of atoms can participate in the cooperative motion and the shearing path should be longer. The effect of raising the reaction temperature is to reduce the length of the shear path because the increased amplitudes of vibrations of the atoms around their equilibrium positions lead to scattering of the standing normal modes of vibration so that the amplitude of these modes are modulated in such a way that their effective shearing path is considerably reduced. Especially effective in reducing the length of shearing paths and indeed preventing the transformation entirely is the presence of interstitial solute atoms which give rise to local potential energy barriers. The extent of the influence of these atoms depends upon the difference between the size of the atom and the size of the interstitial hole. These local distortions also act as scattering centers of the thermal waves and act effectively in suppressing the cooperative movement of solvent atoms over any significant range.

Thus from the above arguments, it is clear why pro-eutectoid ferrite formed in steels at higher transformation temperatures can assume various morphologies. It is planned to present a formalized analysis of various aspects of shear transformations in a future report.

P. SUMMARY

(1) The chemistry of boron and the metallurgy of boron in iron and steel is thoroughly reviewed.

(2) On the basis of critical evaluation of the existing information on the boron hardenability effect, a working hypothesis for the mechanism of the boron has been evolved. The essential features of the hypothesis are the following:

(a) The effect of boron in steels is the retardation of the formation of pro-eutectoid ferrite and upper bainite. Boron does not retard the formation of pearlite.

(b) Adsorption effects of boron at austenite grain boundaries is very likely an important factor in the hardenability effect.

(c) Important chemical interactions between carbon and boron in austenite are unlikely.

(d) It is concluded that pro-eutectoid ferrite forms from austenite by a shear mechanism.

(e) The boron hardenability effect is a solid solution effect. The high strain energy peaks in austenite associated with the boron atoms are effective in retarding the shear formation of ferrite.

(f) Fundamentally, carbon, nitrogen, and boron affect hardenability by the same mechanism, but boron is considerably more effective than carbon and nitrogen.

(g) The strain energy peaks associated with carbon, nitrogen, and boron atoms were calculated and were found to be in the ratio 1:2:10.

(h) A shear transformation occurs by a cooperative movement of several atoms whereas in diffusion the atoms change their positions at random and independently.

(i) The source of shear in allotropic transformations are shearing movements associated with the normal modes of thermal vibrations of the crystal. The higher the temperature of transformation, the shorter the individual shearing path.

(j) As a general principle, a nucleation and growth process takes place when the system passes from a disordered state to a more highly ordered state; shear transformation involves cooperative movement from one ordered state to another ordered state.

BIBLIOGRAPHY

1. Guillet, L., "Boron Steels," Jnl. Iron and Steel Inst., No. 2, 207-218 (1907).

2. Gillett, H. W., Mack, E. L., "Experiments with Rare Elements in Steels," Trans. Electrochem. Soc., 43, 231-259 (1923).

3. Walters, Richard, U. S. Patent 1,509,624 Sept. 23 (1924); U. S. Patent 1,519,388 Dec. 16 (1924).

4. Archer, R. S., "Boron in Steel," Metal Progress, 55, 677 (1946).

5. Nicholson, M. E., "Solid Solubility of Boron in Iron," Jnl. of Metals, 148 (Feb. 1952).

6. Nicholson, M. E., Private communication.

7. Laubengayer, A. W., Newkirk, A. E., Brenaur, R. L., "Progress in the Preparation and Determination of the Properties of Boron," Jnl. Chem. Education, 19, 382-5 (1942).

8. Laubengayer, A. W., Hurd, D. T., Newkirk, A. E., Hoard, J. L., "Preparation and Properties of Pure Crystalline Boron," Jnl. Am. Chem. Soc. 65 1924-31 (1943).

9. Hoard, J. L., Geller, S., Hughes, R. E., "Communication to the Editor," pertaining to the elementary structure of boron, Jnl. Am. Chem. Soc., 73, 1892 (Ap. 1951).

10. Johnston, H. L., Hersh, H. N., Kerr, E. C., "V. Heat Capacity of Pure Elementary Boron in Both Amorphous and Crystalline Conditions Between 13 and 305°K," Jnl. Am. Chem. Soc., 73, 1112 (1951)

11. Godfrey, T. N., Warren, B. E., "The Coordinate Scheme in Crystalline Boron," Jnl. Chem. Phys., 18, 1121-2 (1950).

12. Wells, A. F., Structural Inorganic Chemistry, Oxford Univ. Press, p. 488.

13. Seitz, F., The Physics of Metals, McGraw-Hill, p. 29 (1943).

14. Kiessling, R., "The Borides of Some Transition Elements," Jnl. of Electrochem. Soc., 98, 166-9 (1951).

15. Hagg, G., "Regularity in Crystal Structure in Hydrides, Borides, Carbides, and Nitrides of Transition Elements," Z. physik. Chem., 12, 33-56 (1931).

16. Norton, J. T., Blumenthal, H., Sindeband, S. J., "Structure of Diborides of Ti, Zr, Cb, Ta, and V," AIMME Trans., 185, 749 (1949).

17. Hannesen, G., "Iron-Boron System," Z. anorg. Chem., 89, 257 (1914).

18. Tschischewski, N., Herdt, A., " Iron-Boron Alloys," Jnl. Russ. Met. Soc., 1, 533 (1915). Abstracted in Jul. Iron Steel Inst., Bd., 96 S451 (1917).

19. Hausen, Max, Der Aufbar der Zweistofflegierungen, published by Edwards Bros., Inc., Ann Arbor, Mich., 271 (1943).

20. Wever, F., Mueller, A., "Concerning the Binary Iron-Boron System and the Structure of Iron-Boride," Z anorg. allgem Chem., 192, 317 (1930).

21. Bjurstrom, T., Arnfelt, H., "Iron-Boron System," Z. physik. Chem, B4, 469 (1929).

22. Wasmuht, R., "Iron-Boron Alloys and 18-8 Steel Plus Boron," Metals and Alloys, 3, 105-10 (1932).

23. Vogel, R., Tammann, G., "Concerning the Fe-C-B Ternary Diagram," Z. anorg. allgem. Chem., 123, 225 (1922).

24. Clark, D. S., "Metallographic Investigation of the Iron, Iron-Carbide, Iron-Boride System," Ph.D. Thesis, California Institute of Technology, Pasadena, California (1934).

25. Digges, T. G., Irish, C. R., Carwile, N. L., "Effect of Boron on the Hardenability of High-Purity Alloys and Commercial Steels," J. Research Nat'L. Bur. Stand., 41, 545-74 (1948). Research Paper #1938.

26. Campbell, T. D., Fay, H., "The Case Hardening of Steel by Boron and Nitrogen," Ind. Eng. Chem., 16, 719 (1924).

27. Wells, C., et al., Second Quarterly Report (WAL 730/454-7) O. O. Project No. TR3-3002A. Carnegie Institute of Technology, Pittsburgh, Pa. Jan. 1, 1948.

28. This reference has been deleted.

29. Kase, T., "Cementation of Boron on Some Metals," abstracted in Metals and Alloys, 9, 661 (1938).

30. Cornelius, H., Bollenrath, F., "The Effect of Carbon on the Diffusion of Some Elements in Steel," Arch. Eisenhuttenw., 15, 145-52 (1941).

31. Wells, C. Batz, W., Mehl, R. F., "Diffusion Coefficient of Carbon in Austenite," AIMME Trans., 188, 553 (1950).

32. Seith, W., Daur., T., "Electrical Transport in Solid Alloys," Z. Elecktrochem., 44, 256-60 (1938).

33. Dayal, P., Darken, L. S., "Migration of Carbon in Steel Under the Influence of Direct Current," AIMME Trans., 188, 1156 (1950).

34. Darken, L. S., "Diffusion of Carbon in Austenite with a Discontinuity in Composition," AIMME, Inst. Metals Div., Metals Tech., 15, #6, T.P. #2443 (1948).

35. Blanter, M. E., "Effect of the Nickel Content on the Diffusion of Carbon in Austenite," Zhur. Tekh. Fiz, 20, 217-21 (1950). Abstracted in Chem. Abstracts (1951).

36. Ham, J. L., Parke, R. M., Hersig, A. J., "The Effect of Molybdenum on the Rate of Diffusion of Carbon in Austenite," ASM Trans., 31, 877 (1943).

37. Smoluchowski, R., "Diffusion Rates in Fe-Mo and Fe-W Alloys," Phys. Rev. 63, 438-40 (1943).

38. Udy, M. C., Rosenthal, D. C., "Boron in Certain Alloy Steels," T. P. 2085, Metals Tech., Oct., 1946.

39. Panel on Substitution of Alloying Elements in Engineering Steels, "Boron Steels," Metal Progress, Aug. (1951).

40. Anon., "Saving Alloys in Steel by Using Addition Agents," Metal Progress, 42, 1061-9 (1942).

41. Digges, T. G., Reinhart, F. M., "Influence of Boron on Some Properties of Experimental and Commercial Steels," J. Research, Nat'l. Bur. Standards, 39, 67-131 (1947).

42. Imai, Y., Imai, H., "An Investigation on Boron Treated Steels: I. On the Hardenability of Boron Treated Medium-Carbon Steels, Especially the Effect of Nitrogen Content in Steels," Science Reports of the Research Institute, Tohaka Univ., Sec. A, 2, 260 April (1950).

43. Day, M. J., "Thermally Hardenable Boron-Titanium Steels," U. S. Patent 2,528,867, Nov. 7, 1950.

44. Gurry, R. W., "The Relative Deoxidizing Power of Boron in Liquid Steel and the Elimination of Boron in Open Hearth Process," AIMME T.P. #1641 (1943).

45. Derge, G., "The Boron-Oxygen Equilibrium in Liquid Iron," AIMME Trans., 167, 93 (1946).

46. Chipman, J., "Another Look at the Problem of Steel Deoxidation," Metals Progress, 56, 211-21 (1949).

47. Kelley, K. K., "Contributions to the Data on Theoretical Metallurgy; VIII. The Thermodynamic Properties of Metal Carbides and Nitrides," Bur. of Mines, Bull, 407 (1937).

48. Thompson, M. de Kay, "The Total and Free Energies of Formation of the Oxides of Thirty-Two Metals," published by The Electrochemical Society, Inc., N. Y., (1942).

49. Southard, J. C., "The Thermal Properties of Crystalline and Glassy Boron Trioxide," J. Am. Chem. Soc., 63, 3147 (1941).

50. Smithells, C. J., Metals Reference Handbook, Interscience Publishers, Inc., New York, N. Y., 428-33 (1949).

51. Grange, R. A., Seens, W. B., Holt, W. S., Garvey, T. M., "Effect of Boron and Kind of Boron Addition Upon the Properties of Steel," ASM Trans., 42, 75 (1950).

52. Anon., "Low Cost Boron Elevates Steel Properties," Soc. Auto. Engr. J., 55, 65 (1947).

53. Comstock, G. F., "Effect of Eight Complex Deoxidizers on Some Properties of 0.40% Carbon Forging Steels," AIMME Trans., 150, 408-20 (1942).

54. Corbett, R. B., Williams, A. J., "Effect of Boron in Steel," U. S. Bur. of Mines, Dept. Investigations 3816 (1945).

55. Metals Handbook, Published by ASM, Cleveland, Ohio, 489 (1948).

56. Grossman, M. A., "Hardenability Calculated from Chemical Composition," AIMME Trans., 150, 227-59 (1942).

57. Welchner, J., Rowland, E. R., Ubben, J. E., "Effect of Time, Temperature and Prior Structure on the Hardenability of Several Alloy Steels," ASM Trans., 321, 521 (1944).

58. Rowland, E. S., Welchner, J., Marshall, R. H., "Effect of Several Variables on the Hardenability of High Carbon Steels, AIMME Trans., 158, 168-179 (1944).

59. Kramer, J. R., Siegel, S., Brooks, J., "Factors for the Calculation of Hardenability," AIMME, T.P. #2029, Metals Tech. June (1946).

60. Crafts, W., Lamont, J. S., "Effect of Some Elements on Hardenability," AIMME, T. P. #1657, Metals Tech., Oct. (1946).

61. Kramer, J. R., Hafner, R. H., Toleman, S. L., "Effect of Sixteen Alloying Elements on Hardenability of Steel," AIMME, T.P. #1636 (1943).

62. Glen, J., "The Effect of the Major Alloying Elements and of Boron on the Hardenability of Steel," Iron & Steel Inst., Symposium on Hardenability, 356-400 (1946).

63. Grange, R. A., Garvey, T. M., "Factors Affecting the Hardenability of Boron-Treated Steels," ASM Trans., 37, 136 (1946).

64. Rahrer, G. D., Armstrong, C. D., "The Effect of Carbon Content on the Hardenability of Boron Steels," ASM Trans., 40, 1099 (1948).

65. Dean, R. S., Silkes, B., "Boron in Iron and Steel," U. S. Bur. of Mines, Information Circular 7363, 56 pp. (1946).

66. Potaszkin, R., "Influence of Small Boron Additions on the Properties of Carbon Steel," Revue de Met., 47, 55-87 (1950).

67. Potaszkin, R., Jaspart, M., "Second Report of the Committee on Boron Steels," Revue de Met., 48, 379-412 (1951).

68. Brik, S. D., Neimark, V. E., Entin, R. I., "Effect of Boron and Vanadium on the Kinetics of the Isothermal Transformation of Austenite," Stal., 6, 661-6 (1946); Abstracted in Chemical Abstracts (1947).

69. United States Steel Corporation, "Atlas of Isothermal Transformation Diagrams" (1951).

70. "Boron Steel," Published by ASM, Cleveland, Ohio (1952).

71. Schwartz, H. A., "Boron as an Accelerator of Malleable Annealing," Foundry, 72, 129, 182 (1944).

72. Eckman, H. A., Maack, H. W., U. S. Patent #2,450,395, Sept. (1948).

73. Joly, G., "Influence of Chromium on Graphitization of White Cast Iron," Am. Foundryman, 14, 60-64 (1948).

74. Krynitsky, A. I., Stern, H., "Effect of Boron on the Structure and Some Physical Properties of Plain Cast Irons," J. Research Nat'l. Bur. of Standards, 42, 465-79 (1949).

75. Micksch, J. E., Fabert, H. A., Cover, G. M., "Effect of Boron Additions on Malleabilization of White Cast Iron," Am. Foundryman, 14 30-7 (1948).

76. Mellor, J. W., A Comprehensive Treatise on Inorganic and Theoretical Chemistry, Vol. V, pp. 12-13.

77. Yensen, T. D., "The Effect of Boron Upon the Magnetic and Other Properties of Electrolytic Iron Melted in Vacuo," University of Illinois Bull. No. 77, Engineering Experiment Station, 1915.

78. Boss, G. H., "Is Hardenability of Boron Steels Indirectly Due to Complete Deoxidations?" Metals Progress, 51, 265 (1947).

79. Chandler, H. T., Bredig , M. A. Discussion of Reference 63. ASM Trans. 37, 136 (1946).

80. Spretnak, J. W., Speiser, Rudolph, "Grain and Grain Boundary Compositions: Mechanism of Temper Brittleness," ASM Trans., 43, 734-47 (1951).

81. Corson, M. G., Discussion of Reference 63.

82. Anon, "Boron in Steels," Metals and Alloys, 17, 1228 (1943).

83. Udy, M. C., "Boron in Steel: Principles and Practice." Paper presented at the Electric Furnace Steel Conference, Pittsburgh, Pa., Dec. (1951).

84. Bardgelt, W. E., Reeve, L., "Mechanical Properties of Low Carbon-Low Alloy Steels Containing Boron," Jnl. of Iron and Steel Inst., 163, 277 (1949).

85. United States Steel Corporation, "Atlas of Isothermal Transformation Diagrams," 121-128 (1951).

86. Phillips, A., Brick, R. M., "Grain Boundary Effects as a Factor in Heterogeneous Equilibrium of Alloy Systems," Jnl. Franklin Inst., 215, 557 (1933).

87. Dean, G. R., Davey, W. P., "Solubility of Copper in the Grain Boundary Material of a Solid Solution of Copper in Zinc," ASM Trans., 26, 267 (1938).

88. Smith, R. P., "Equilibrium of Iron-Carbon Alloys with Mixtures of $CO-CO_2$ and CH_4-H_2," Jnl. Am. Chem. Soc., 68, 1163 (1946).

89. Gudtsov, N. T., Nazarov, T-N, "Influence of Boron Upon the Kinetics of the Austenite Transformation in Steel," Izvestiya Akademii Nauk SSSR, Otd. Tekh. Nauk, No. 3 (1950); Brutcher Translation No. 2617.

90. Johnson, W. A., Mehl, R. F., "Reaction Kinetics in Processes of Nucleation and Growth," AIMME Trans., 135, 416 (1939).

91. Hull, F. C., Colton, R. A., Mehl, R. F., "Rate of Nucleation and Rate of Growth of Pearlite," AIMME Trans., 150, 185 (1942).

92. Johnson, W. A., Discussion of reference 91, p. 208.

93. Mehl, R. F., "The Decomposition of Austenite by Nucleation and Growth Processes," Jnl. Iron and Steel Inst., June (1948).

94. Cohen, M., Machlin, E. S., Paranjpe, V. G., "Thermodynamics of the Martensite Transformation," ASM Trans., 42A, 242, (1950).

95. Blanchard, J. R., Parke, R. M., Herzig, A. J., "The Effect of Molybdenum on the Isothermal Subcritical Transformation of Austenite in Low and Medium Carbon Steels," ASM Trans., 29, 317 (1941).

96. Bowman, F. E., Parker, R. M., "The Partition of Molybdenum in Iron-Carbon-Molybdenum Alloys at 1300 Degrees Fahr. and the Nature of the Carbides Formed," ASM Trans., 33, 481 (1944).

97. Bowman, F. E., "The Partition of Molybdenum in Steel and Its Relation to Hardenability," ASM Trans., 35, 112 (1945).

98. Ham, J. L., "The Rate of Diffusion of Molybdenum in Austenite and Ferrite," ASM Trans., 35, 331 (1945).

99. Bowman, F. E., "Partition of Molybdenum in Hypoeutectoid Iron-Carbon-Molybdenum Alloys," ASM Trans., 36, 61 (1946).

100. Hultgren, A., "Isothermal Transformation of Austenite," ASM Trans., 39, 915 (1947).

101. Mehl, R. F., Smith, D. W., "Studies Upon the Widmanstätten Structure, Part V, The Gamma-Alpha Transformation in Pure Iron," AIMME Trans., 113, 203 (1934).

102. Mehl, R. F., Barrett, C. S., Smith, D. W., "Studies Upon the Widmanstatten Structure, Part IV, The Iron-Carbon Alloys," AIMME Trans., 105, 215 (1933).

103. Smith, G. V., Mehl, R. F., "Lattice Relationships in Decomposition of Austenite to Pearlite, Bainite, and Martensite," AIMME Trans, 150, 210 (1942).

104. McBride, D. L., Herty, C. H. Jr., Mehl, R. F., "The Effect of Deoxidation on the Rate of Formation of Ferrite in Commercial Steels," ASM Trans., 24, 281 (1936).

105. Kulin, S. A., Speich, G. R., "Isothermal Martensite Formation in an Iron-Chromium-Nickel Alloy," Jnl. of Metals, p. 258, March (1951).

106. Nehrenberg, A. E., "Growth of Austenite as Related to Prior Structure," AIMME Trans., 188, 162 (1950).

107. Kurdjumow, G. V., discussion of reference 102.

108. Bose, B. N., Hawkes, M. F., "Kinetics of the Eutectoid Transformation in Alloys of Iron and Nitrogen," AIMME Trans., 188, 307 (1950).

109. Speiser, R., Spretnak, J. W., Taylor, W. J., "Interstitial Solid Solutions," to be presented to the Journal of Metals (AIMME).

110. Jack, K. H., "The Iron-Nitrogen System: The Preparation and the Crystal Structure of Nitrogen-Austenite (γ) and Nitrogen-Martensite (α')," Proc. Royal Soc. A 208,200 (1951).

111. Jack, K. H., "Interatomic Binding Forces in Iron, Cobalt, and Nickel Interstitial Alloys," Ninth Annual Pittsburgh Conference on X-ray and Electron Diffraction, November 29, 30, 1951.